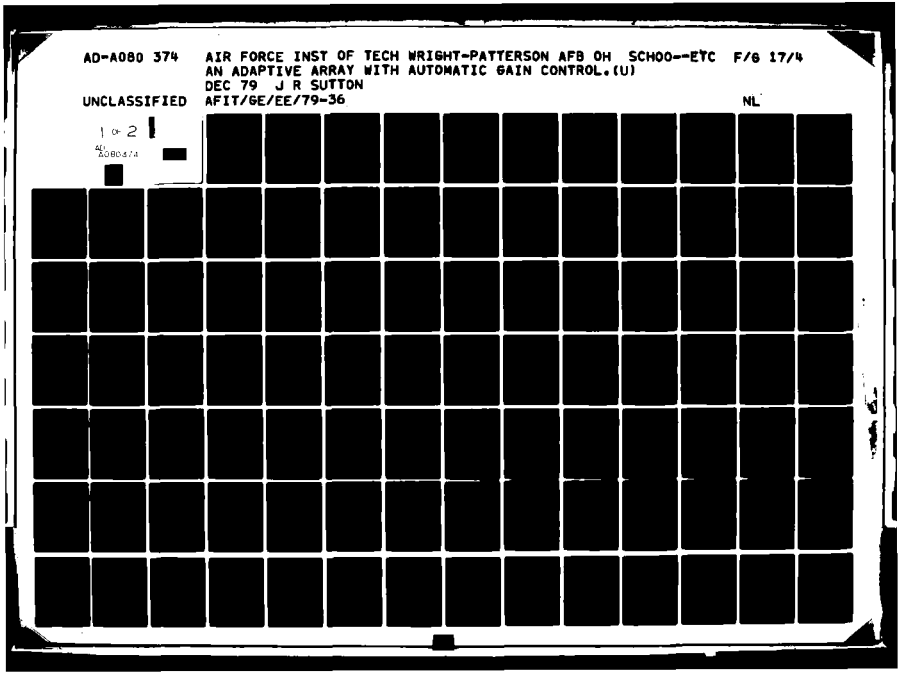
AD-A080 374
AIR FORCE INST OF TECH WRIGHT-PATTERSON AFB OH SCHOO--ETC F/G 17/4
AN ADAPTIVE ARRAY WITH AUTOMATIC GAIN CONTROL.(U)
DEC 79 J R SUTTON
UNCLASSIFIED
AFIT/GE/EE/79-36
NL
1 OF 2
AD A080374

AFIT/GE/EE/79-36

(6) AN ADAPTIVE ARRAY WITH AUTOMATIC GAIN CONTROL,

(9) Master's THESIS,

(14) AFIT/GE/EE/79-36

(10) John Rogers Sutton, Capt, USAF

(11) Dec 79

(12) 98

Approved for public release; distribution unlimited

012225

nt

AFIT/GE/EE/79-36

AN ADAPTIVE ARRAY WITH AUTOMATIC GAIN CONTROL

THESIS

Presented to the Faculty of the School of Engineering
of the Air Force Institute of Technology
Air University
in Partial Fulfillment of the
Requirements for the Degree of
Master of Science

by
John R. Sutton, B.S.E.E.
Capt USAF
Graduate Electrical Engineering
December 1979

Approved for public release; distribution unlimited

Preface

Adaptive arrays are being investigated for use in many communications systems. They appear to be a viable, although expensive, alternative to some anti-jamming systems currently under development. As with all systems the problems associated with signal saturation need addressing and hard limiters are consistently touted as the best form of envelope limiting. Automatic gain controls as envelope limiters are not addressed in much detail; the only claim is to use a "fast" one. Information on the subject appeared sketchy and was chosen for my thesis topic.

Thanks are due to Lt. Colonel Ron Carpinella for his assistance and directions as my advisor. Maripat Meer was most helpful as my typist. My deepest love and appreciation goes to my wife, Leigh, who understood and endured the times we could not be together during the past six months.

John R. Sutton

Contents

List of Figures

List of Tables

Abstract

A three-element adaptive array algorithm with Applebaum-Howells loops combined with a linear automatic gain control (AGC), was analyzed. Computer simulations of array performance for single jammers were presented and analyzed. Jammer scenarios included were: narrowband and broadband, high power, centered and non-centered jammers about the array center frequency, and different automatic gain control response times. No fixed performance criteria were applied to SNR degradation and antenna pattern plots. A non-linear AGC was linearized by expanding the exponential attenuation function in a series and truncating the higher-order terms. The AGC is shown to destroy the typical monotonically decreasing SNR degradation of a constant power, narrow band jammer when its response time is near that of the adaptive loop. Simulation results show that an AGC can cause the adaptive weight amplitudes to vary significantly.

AN ADAPTIVE ARRAY WITH AUTOMATIC GAIN CONTROL

I. Introduction

Background

The analytic theory which describes adaptive antenna arrays is relatively new. Most significant contributions have been made within the last two decades. In the early 1960's, with Howells' development (Ref 1) of IF sidelobe cancelling circuitry, adaptive arrays began to diverge from general RF antenna theory. Further contributions in the 1960's by Applebaum (Ref 2) and Widrow (Ref 3) firmly established the theory of adaptive antenna systems.

The military environment is a natural place for adaptive antenna arrays. In high threat situations intense jamming is expected and adaptive arrays can significantly reduce jamming effects. Adaptive arrays coupled with main beam steering have the capability to shift the inherent antenna pattern nulls to the spatial direction of the interference. Another inherent advantage of analog adaptive arrays is the ability to adapt faster for increasing interference power (Ref 4:21).

Adaptive array theory requires circuitry which performs multiplication. A typical diode mixer performing this operation does not have a large dynamic range. For this reason,

some method of envelope limiting is usually employed in receiver front ends. Hard limiting has been studied in depth by Gabrial (Ref 4) and Brennan and Reed (Ref 5). The study of other envelope limiters has not been investigated in depth; probably due to the non-linear nature of the implementing devices.

Objectives

This thesis will examine the performance of a maximum signal to noise ratio array algorithm which incorporates an automatic gain control (AGC). The present literature only specifies the use of "fast" AGC circuits. The question then is how "fast" an AGC is required. Real time simulation of an AGC/array system can provide insight into these questions. A comparison study of the simulations will hopefully show any relationships which need to be addressed in the design of future military systems.

Assumptions

At the outset it is assumed that all system models are narrowband with bandwidth no greater than ten percent of center frequency. It is also assumed that the adaptive array is steered in the direction of the desired signal. The last major assumption concerns intermodulation distortion. It is a well known fact that intermodulation products are generated at the output of a bandpass non-linearity. These products

are frequency dependent and demand a full non-linear analysis of the system in question. For purposes of this thesis these products are assumed to be zero everywhere. This simplification will allow analysis of the AGC in the linear domain. Since a relationship between the power dependence of the array and the AGC is only desired, investigation of small intermodulation would probably be of no consequence to the results. Hence, this assumption is not out of line with the required analysis.

Approach

The approach in this thesis is to present models for both the adaptive array and AGC. These models will form the algorithm to simulate transient response. SNR degradation will be the principle array performance measure. A comparison study of array performance for different AGC response time constants and jammer powers will be conducted.

Because of the tutorial treatment by Gabriel (Ref 4) on adaptive arrays and their performance, his model, with few exceptions, is used as the foundation for this thesis. The next section contains the adaptive array model.

II. Adaptive Array Model

Beginning Concepts

An understanding of phase conjugacy, space factor, retrodirectivity, interferometers, and integrating filters provides important insight into the operation of an adaptive array model.

Phase Conjugacy and Retrodirectivity. An adaptive array performs spatial filtering by sensing the direction of an interference source and forming a retrodirective beam. This retrodirective beam is formed from the jammer's spatial dependent, uniform phase shift along the array elements. In a sense, the retrodirective beam is subtracted from the unadapted pattern to alleviate some of the jammer's effects. Figure 1 is a representation of this process. Signal multiplication (mixing) is used to derive the necessary conjugate phase to create the beam.

This conjugate phase relationship is derived by multiplying (mixing) the received signal with a reference signal of equal or higher frequency. To illustrate this principle define complex (denoted by the overbar) signals $\overline{E}_1$ and $\overline{E}_2$ as

$$\overline{E}_1 = A_1 e^{j(\omega_1 t + \phi_1)}$$

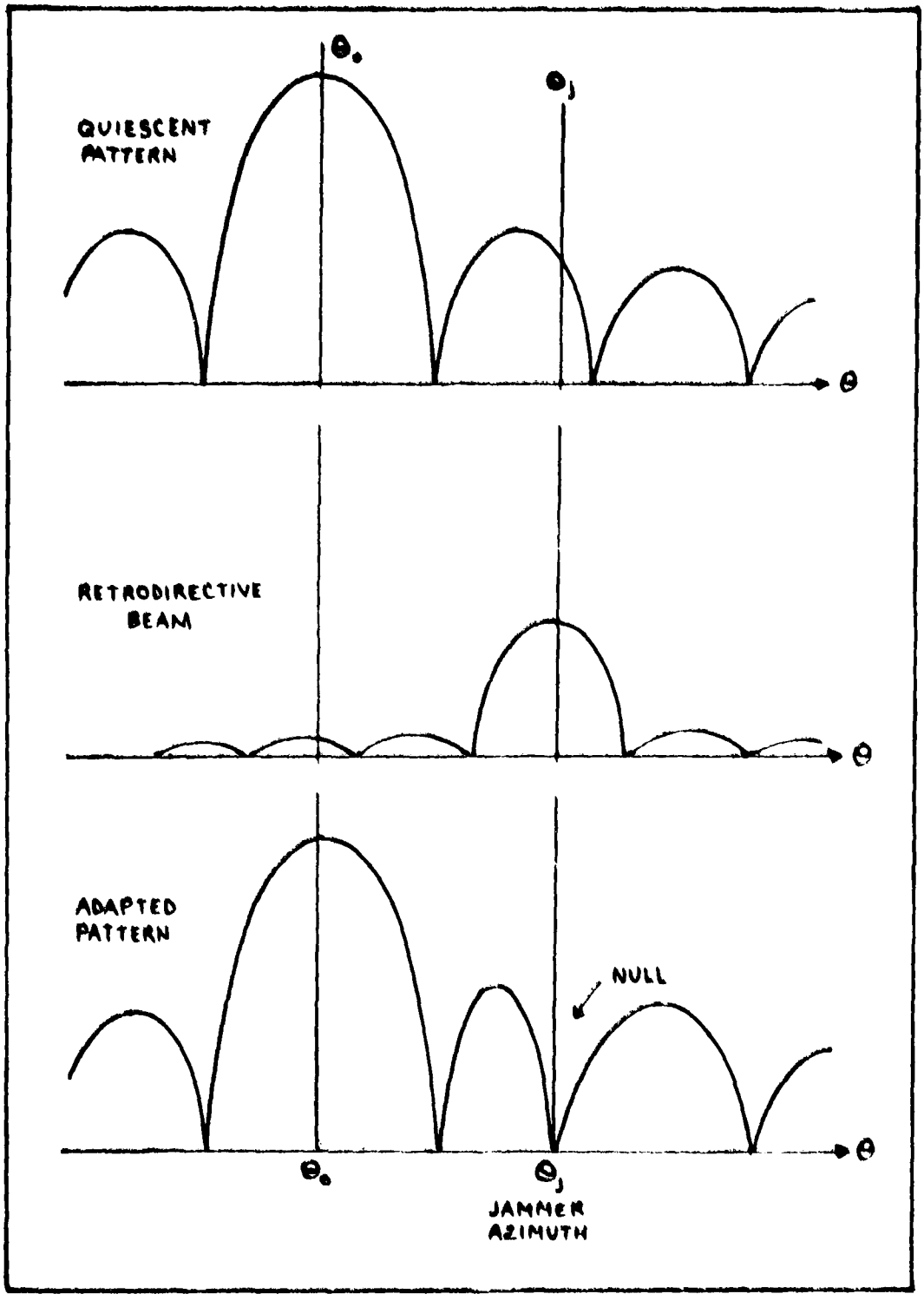

Figure 1. Retrodirective Beam Nulling Principle

and

$$\bar{E}_2 = A_2 e^{j(\omega_2 t + \phi_2)}$$

The product of their real parts is then

$$E_1 E_2 = A_1 A_2 \cos(\omega_1 t + \phi_1)\cos(\omega_2 t + \phi_2)$$

$$E_1 E_2 = \tfrac{1}{2} Re(\bar{E}_1 \bar{E}_2) + \tfrac{1}{2} Re(\bar{E}_1 \bar{E}_2^*) \qquad (1)$$

where the asterisk indicates complex conjugate. If $\bar{E}_2$ is considered an incoming signal and $\bar{E}_1$ a reference signal then Eq(1) shows that a phase conjugate relationship can be isolated. This is accomplished by choosing the difference frequency component at the output with a bandpass filter. Note the required relationship ($\omega_1 \geq \omega_2$) for the operation to make sense in the frequency domain.

Antenna Array Space Factor. A uniform linear array of several identical antenna elements is usually specified, in a general sense, by array gain as a function of azimuth. This "pattern" is also called the space factor and can be through of as a type of gain transfer function for the array. By superposition of an odd number of equally spaced (in distance and electrical phase) elements it can be shown that the space factor is (Ref6:74)

$$G(u) = A_0 \sum_{n=-\frac{1}{2}(N-1)}^{n=\frac{1}{2}(N-1)} e^{jnu} \qquad (2)$$

where A_0 is the element current amplitude, N, the number of elements, and u, the uniform phase shift. u can be further defined as a path length phase difference associated with far field source at angle θ from the normal to the array.

$$u = \frac{2\pi d}{\lambda} \sin\theta \qquad (3)$$

where d is the distance between antenna elements. This geometric relationship is shown in Figure 2 for three elements. Since Eq(2) is a geometric series in e^{ju} it can be reduced to

$$G(\theta) = A_0 e^{-\frac{1}{2}(N-1)ju} \left(\frac{e^{jNu}-1}{e^{ju}-1}\right)$$

$$G(\theta) = A_0 \frac{\sin\frac{Nu}{2}}{\sin\frac{u}{2}} \qquad (4)$$

For this paper Eq(4) with $A_0=1$ is the unadapted or quiescent antenna pattern.

$$G_q(\theta) = \left| \frac{\sin\left(\frac{N\pi}{2}\sin\theta\right)}{\sin\left(\frac{\pi}{2}\sin\theta\right)} \right| \qquad (5)$$

where $d=\frac{\lambda}{2}$.

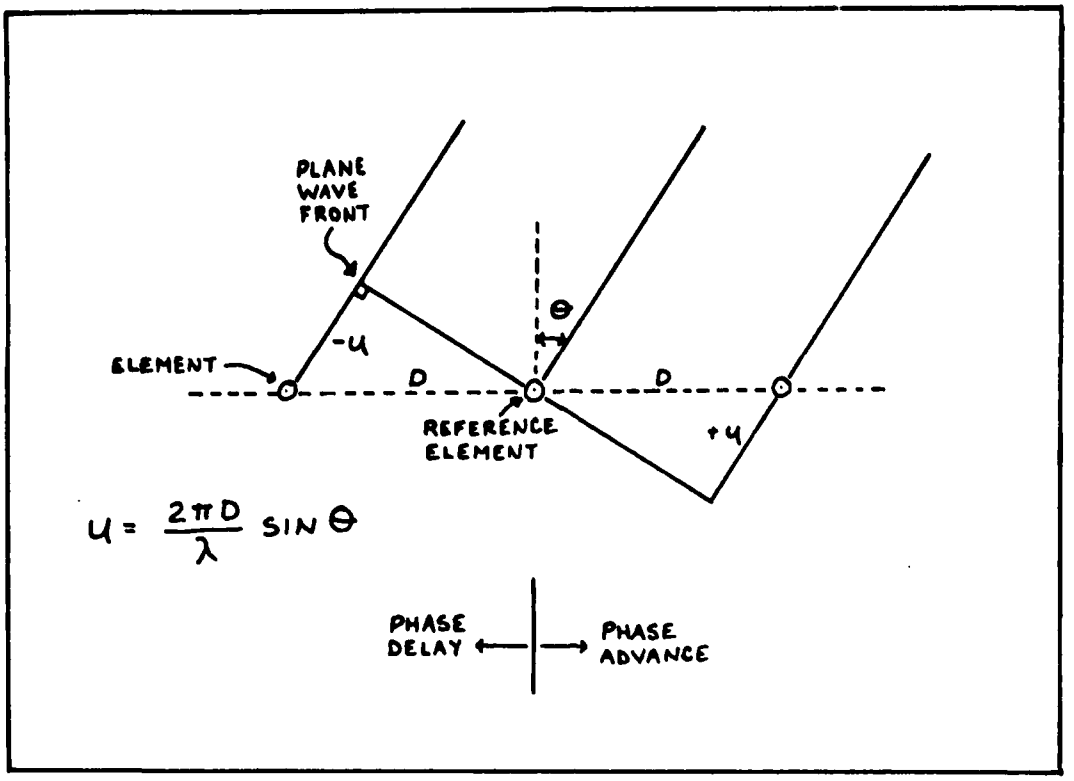

Figure 2 Geometric Interpretation of Phase Factor

Cross Correlation Interferometer. Insight into the operation of an adaptive array can be found by examining a cross-correlation interferometer (Ref4:5-8). This principle is used in radar and radio astronomy to extract spatial information from received signals. An adaptive array uses the interferometer principle to derive phase conjugate element "weights" for forming a retrodirective beam. The received signal is cross-correlated with a reference signal and filtered to estimate the value of the cross-correlation. Figure 3 is a schematic of a cross correlation interferometer.

RF signals arrive at antennas A and B with a path length

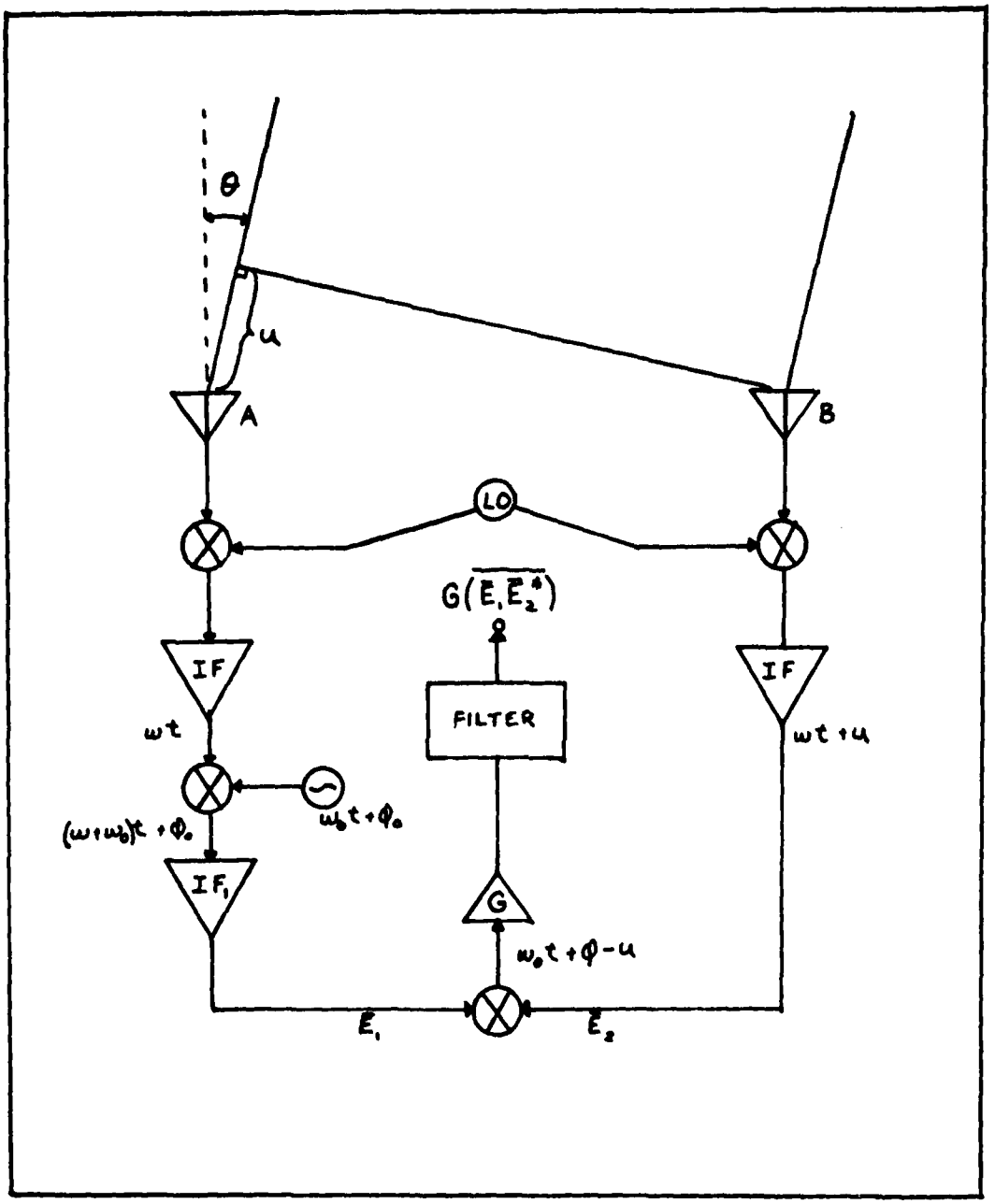

Figure 3 Cross Correlation Interferometer

phase difference u as defined in Eq(3) and are translated to IF.

IF translation must preserve the RF phases and amplitudes.

The real part of the IF signal from antenna B can be written as

$$E_2 = b\cos(\omega t + u) \tag{6}$$

where b is the amplitude, ω, the IF frequency and, u, the phase advance at B relative to A. The IF signal from A is then offset to a higher frequency by mixing with constant reference frequency ω_0. Thus,

$$E_1 = a\cos[(\omega + \omega_0)t + \phi_0] \tag{7}$$

where ϕ_0 is the phase constant of the reference. If E_1 and E_2 are mixed as in the previous section the output of the mixer is a true cross-correlation of the received signals at a carrier frequency ω_0.

$$Re[\bar{E}_1\bar{E}_2^*] = \frac{ab}{2}\cos(\omega_0 t + \phi_0 - u) \tag{8}$$

The combined signal is then amplified and integrated in a narrowband filter to improve the output signal-to-noise ratio. This filtering operation can also be thought of as an averaging and is very important to the array operation.

$$\int_t^{t+T} Re[\bar{E}_1\bar{E}_2^*]\,dt = Re(\overline{\bar{E}_1\bar{E}_2^*}) \tag{9}$$

The averaged output is called complex weight W. It is defined as

$$\overline{W} = G\left(\bar{E}_1, \bar{E}_2^*\right) \tag{10}$$

and

$$W = Re[\overline{W}] = Gab\cos\left(\omega_0 t + \phi_0 - u\right) \tag{11}$$

$\overline{W}$ can be further mixed with $\bar{E}_2$ and the sum frequency, $\bar{E}_3$, chosen so that

$$\bar{E}_3 = \overline{W}\bar{E}_2 = G\left(\bar{E}_1, \bar{E}_2^*\right)\bar{E}_2 \tag{12}$$

Since $\bar{E}_2$ is a sinusoid with no modulation

$$\bar{E}_3 = G\left|\bar{E}_2\right|^2 E_1 \tag{13}$$

or

$$E_3 = Re[E_3] = b^2 Ga\cos[(\omega_0+\omega)t + \phi_0] \tag{14}$$

Note that the phase of $\bar{E}_2$ is cancelled and $\bar{E}_3$ is now in phase with $\bar{E}_1$. In general, where $\bar{E}_1$ and $\bar{E}_2$ are broadband envelope-modulated signals, u is different for each spectral line and weight $\overline{W}$ represents an average conjugate phase. Thus $(\overline{W}\bar{E}_2)$ would not result in complete phase cancellation across the channel band.

Integrating Filter. The averaging noted in the previous section is accomplished by a simple RC filter. A choice of

a RC filter over RLC type filters is based upon unwanted phase properties of the RLC filter (Ref4:10). To use the simple RC filter it becomes necessary to convert from offset frequency ω_0 to dc baseband in-phase and quadrature channels, use the RC filters, and then remodulate back to the offset frequency prior to mixing. Since a RC filter has been used, the following differential equation specifies its transient response:

$$\frac{W}{R} + C\frac{dW}{dt} = \frac{v}{R}$$

or

$$\tau_0 \frac{dW}{dt} + W = v \tag{15}$$

where τ_0=RC and v is an input voltage. Using Laplace transform analysis Eq(15) becomes

$$\overline{W} = \left(\overline{W}(0) - \overline{v}_0\right) e^{-\alpha t} + \overline{v}_0 \tag{16}$$

where $\alpha = \frac{1}{\tau_0} = \frac{1}{RC}$

Previously it was stated that this filter operation was important to adaptive array operation. Without this filter to provide integration, the output can not be considered a cross-correlation of the two input signals. Up to this point all inputs have been deterministic sinusoids and the cross correlation is the time average of the multiplied inputs

(Ref 7:46). This is represented as

$$R_{xy}(\tau) = \lim_{T\to\infty} \frac{1}{2T}\int_{-T}^{T} x(t)\, y(t+\tau)\, dt \qquad 17$$

In reality, signal y is a delayed version of signal x and Eq(17) is more properly an autocorrelation of a deterministic sinusoid. Since the signals are still considered sinusoidal, the time average can be taken over one period, T_0, such that

$$R_x(\tau) = \frac{1}{T_0}\int x(t)\, x(t+\tau)\, dt \qquad 18$$

These relationships can be expanded to random processes where the signals are now complex envelopes. If τ, the integration time is long compared to the inverse of the IF frequency, then the limit to infinity in Eq(17) is adequately approximated. Further, if ergodicity of the process is assumed (Ref 8:329), time averages can be considered equal to ensemble averages and

$$\int_{t}^{t+T} (\bar{E}_1 \bar{E}_2^*)\, dt = E\{\bar{E}_1 \bar{E}_2^*\} = \overline{\bar{E}_1 \bar{E}_2^*} \qquad 19$$

where $E\{\cdot\}$ denotes expectation (Ensemble average). The term cross-correlation is now properly used because the two signals, although not independent, are processes from different antenna elements.

Two-Element Array

A simple two-element adaptive array using one Applebaum-Howells loop with beam steering is shown in Figure 4. For simplicity, the local oscillator, IF amplifiers, and bandpass filters are not included. They are not essential to the analysis. Beam-steering signals B_1^* and B_2^* have been added to steer the receive beam in some desired azimuth direction θ_0 . For the analysis these signals are constant and θ_0 is considered to be broadside to the array (0 degrees). These signals are input at some reference offset ω_0 . To simplify the notation in the following equations, all signals are assumed to be carrier modulated. Hence, the bandlimited spectra are represented by their complex envelopes and any modulation will not appear explicitly. Gain G shall be set at unity for the time being.

When no interference is present adaptive weight W_2 will settle to a value commensurate with receiver noise. This quiescent weight is denoted by W_q . To point the beam in direction θ_0 under quiescent conditions

$$W_1 = e^{ju_0} \quad \text{and} \quad W_q = W_1^* = e^{-ju_0} \tag{20}$$

where

$$u_0 = \frac{\pi d}{\lambda} \sin \theta_0 \tag{21}$$

Weight W_1 is injected as B_1^*. B_2^* is related to W_q by b_2 so

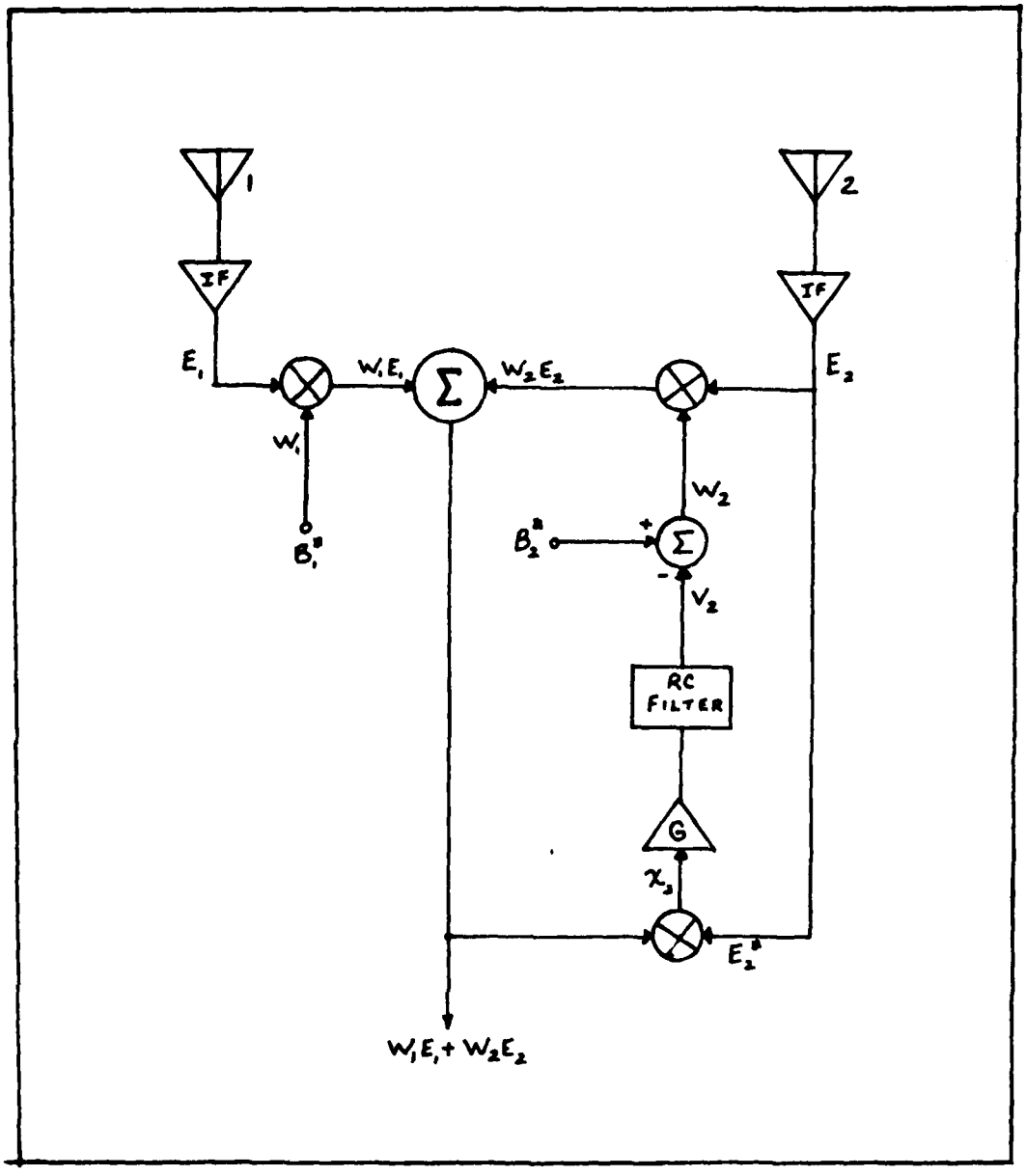

Figure 4 Two Element Adaptive Array

$$B_2^* = b_2 W_2 = b_2 e^{-j\psi_2} \tag{22}$$

Further define

$$E_1 = n_1 \,, \quad E_2 = n_2 \qquad t<0 \qquad (23)$$

$$E_1 = n_1 + J_i e^{-j\mu_i} \,, \quad E_2 = n_2 + J_i e^{j\mu_i} \qquad t \geq 0 \qquad (24)$$

where receiver quiescent noise n_1 and n_2 are inputs until a statistically independent noise source J_i located at θ_i is turned on at $t=0$. From Figure 4

$$W_2 = B_2^* - V_2 \qquad (25)$$

and

$$x_2 = \left(W_1 E_1 + W_2 E_2\right) E_2^* \qquad (26)$$

After the filtering operation and with Eq(25)

$$\bar{x}_2 = W_1\left(E_1 E_2^*\right) + \left|\bar{E}_2\right|^2 \left(B_2^* - V_2\right) \qquad (27)$$

However, V_2 also obeys the RC filter equation

$$\tau_0 \frac{dV_2}{dt} + V_2 = G\,\bar{x}_2 \qquad (28)$$

Combining Eqs(27) and (28) gives

$$\tau_0 \frac{dV_2}{dt} + \left(1 + \left|\bar{E}_2\right|^2\right) V_2 = \left|\bar{E}_2\right|^2 \left[B_2^* + \frac{W_1\left(\overline{E_1 E_2^*}\right)}{\left|\bar{E}_2\right|^2}\right] \qquad (29)$$

For a step function change in E_1 and E_2

$$V_2(t) = \left[V_2(0) - V_2(\infty) \right] e^{-\alpha t} + V_2(\infty) \tag{30}$$

where

$$V_2(\infty) = \frac{|\bar{E}_2|^2 \left[B_2^* + \frac{W_1 (\overline{E_1 E_2^*})}{|\bar{E}_2|^2} \right]}{1 + |\bar{E}_2|^2} \tag{31}$$

and

$$\alpha = \frac{1 + |\bar{E}_2|^2}{T_0} \tag{32}$$

Eq(30) can be substituted into Eq(25) to get W_2 .

To minimize the output power of the array, $|Y_n|^2$, define W_{02} as the optimum value of W_2 .

$$|Y_n|^2 = |W_1 E_1 + W_2 E_2|^2 \tag{33}$$

If $|Y_n|^2 = 0$ then

$$W_{02} = \frac{-W_1 (\overline{E_1 E_2^*})}{|\bar{E}_2|^2} \tag{34}$$

This form of W_{02} can be used to rewrite Eq(31). Note that W_{02} is the retrodirective weight required to place a spatial pattern null in the direction of interference, θ_0 . Also note that due to the RC filter estimating the cross-correlation, the adaptive process is not instantaneous. The RC filter

is not a perfect integrator with zero bandwidth and some finite settling time will be required to reach steady state for (in this case) a unit step input. The exponential time constant, α , defined in Eq(32) is dependent upon the power in $\bar{E}_2$ and τ_0 . So, while the adaption is not instantaneous, it is power sensitive. Specifically, rewriting Eq(31) with Eq(34) gives

$$V_2(\infty) = \frac{|\bar{E}_2|^2(B_2^* - W_{02})}{1+|\bar{E}_2|^2} \tag{35}$$

For $|\bar{E}_2|^2 \gg 1$

$$V_2(\infty) = B_2^* - W_{02} \tag{36}$$

Combining this with Eq(25) gives

$$W_2(\infty) = W_{02} \tag{37}$$

In summary, without Eq(36)

$$W_2(\infty) = B_2^* - \frac{|\bar{E}_2|^2(B_2^* - W_{02})}{1+|\bar{E}_2|^2} \tag{38}$$

Under quiescent conditions, assuming independent noise voltages in each antenna receiver,

$$\overline{\bar{E}_1 \bar{E}_2^*} = \overline{n_1 n_2^*} = 0 \tag{39}$$

implying that $W_{02}=0$.

Eq(38) then becomes

$$W_2(\infty) = \frac{B_2^*}{1+|n_2|^2} \tag{40}$$

If $B_2^* = b_2 W_q$

$$W_2(\infty) = \frac{b_2 W_q}{1+|n_2|^2} \tag{41}$$

but $W_2(\infty) = W_q$ by definition so

$$b_2 = 1+|n_2|^2 \tag{42}$$

Recall that the amplifier with gain G was set to unity to streamline the analysis.

Realistically,

$$|\bar{E}_2|^2 = G|\bar{E}_2|^2 \tag{43}$$

If, however, G is set to normalize quiescent noise to unity, such that

$$G|n_2|^2 = 1 \tag{44}$$

it is possible to define a ratio, P_i , as interference power to noise power.

$$\frac{G|\bar{E}_2|^2}{G|n_2|^2} = 1 + \frac{|J_i|^2}{|n_2|^2} = 1 + P_i \tag{45}$$

Also define $\mu = G|E_2|^2$ so

$$\mu = 1 + P_i \tag{46}$$

Rewriting the equations necessary to evaluate the weights of the loop in terms of μ gives

$$W_2 = \left[W_2(0) - W_2(\infty) \right] e^{-\alpha t} + W_2(\infty) \tag{48}$$

$$W_2(\infty) = \left[\frac{2}{1+\mu} \right] W_1^* + \left[\frac{\mu}{1+\mu} \right] W_{02} \tag{49}$$

$$W_2(0) = W_0 = W_1^* \tag{50}$$

$$W_{02} = \frac{-W_1}{\mu} P_i e^{-j2\mu_i} \tag{51}$$

$$\alpha = \frac{1+\mu}{T_0} \quad \text{and} \quad \mu = 1 + P_i \tag{52}$$

Gabriel (Ref1:24) gives physical representation to Eq(49) by defining

$$\text{beam-steering component} = \frac{2}{1+\mu} W_1^* \tag{53}$$

$$\text{retrodirective component} = \frac{\mu}{1+\mu} W_{02} \tag{54}$$

and observing that if $P_i << 1$, $W_{02} << 1$ and the beam steering part is dominant. As P_i increases, μ increases such that $\mu >> 1$ and the steering component decreases while the retrodirective dominates.

K-Element Array

Most modern antennas are constructed from many antenna elements to maximize gain and desired directional properties; thus reducing the costs of more expensive items such as receivers and power amplifiers. Practical adaptive arrays should be able to null many interference sources. Since the number of nulls that can be generated by any adaptive array is limited by the number of elements it possesses (Ref4:61) typical arrays have four or more elements. This section analyzes a K-element array with K adaptive loops of the Applebaum-Howells type. Figure 5 is a schematic of such a system. To understand the operation of a K-element adaptive array some basic linear algebra is used. The important equations of the previous section will be generalized to the K-dimensional case.

To begin, define $\underline{E}$ as a k-dimensional column vector such that

$$E_k = n_k + \sum_{i=1}^{I} J_i \, e^{j u_i (2k - K - 1)} \tag{55}$$

and

$$u_i = \frac{\pi d}{\lambda} \sin \theta_i \tag{56}$$

where the lazy underbar indicates matrix quantities. The sources are assumed to be statistically independent. The B_i^*'s

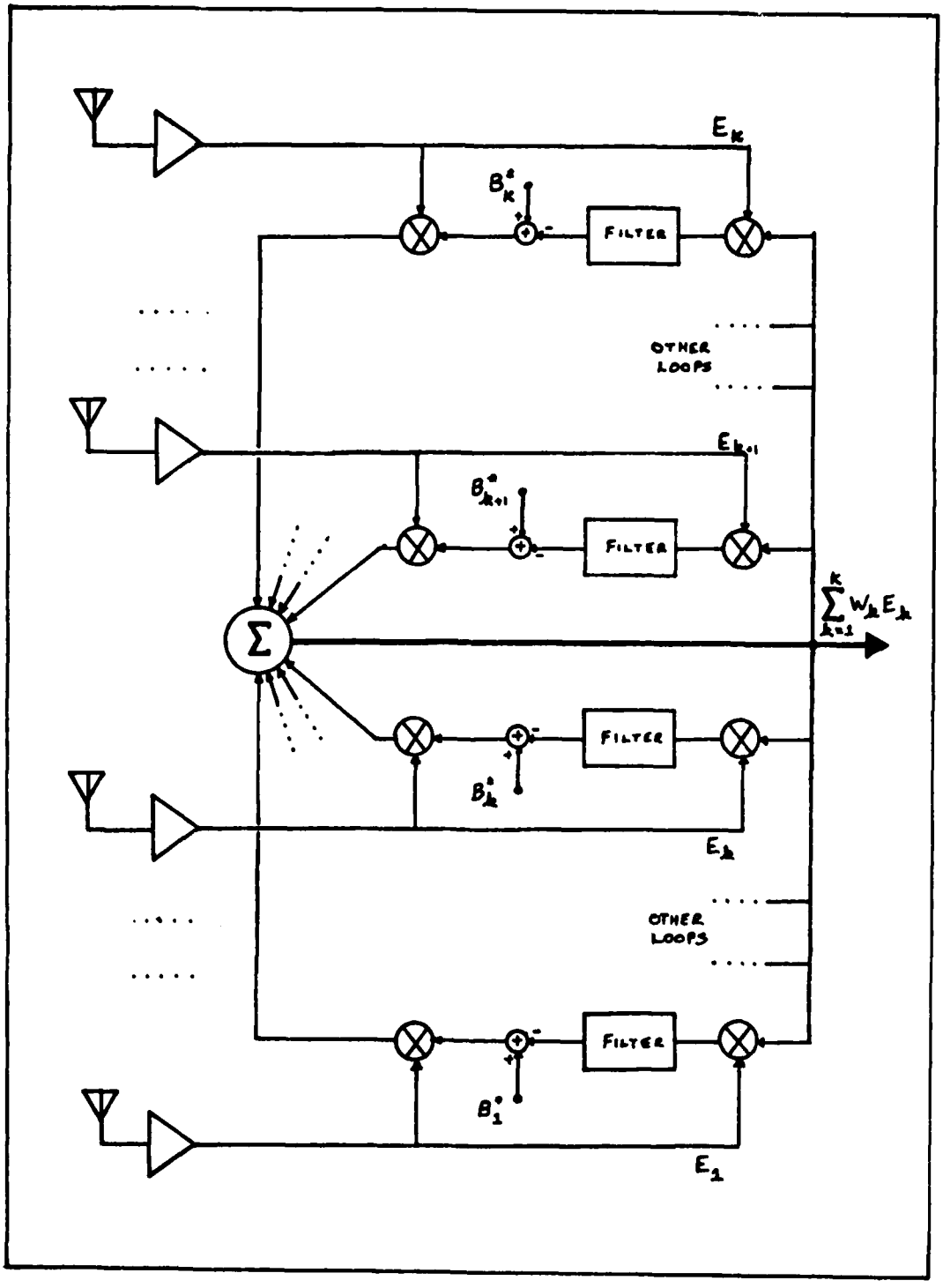

Figure 5. K-Element, K-Loop Adaptive Array

will steer the receive antenna beam in some desired azimuth θ_0 . Therefore quiescent weights W_{qk} should generate the desired quiescent pattern $G_q(\theta)$ as in Eq(5). $\underset{\sim}{W}$ is defined as a k-dimensional colum vector and

$$W_{qk} = a_k e^{-ju_0(2k-K-1)} \tag{57}$$

where

$$u_0 = \frac{\pi d}{\lambda} \sin \theta_0 \tag{58}$$

To be consistent with Eq(4) the a_k's are unity. $\underset{\sim}{S}$ is defined like vectors $\underset{\sim}{E}$ and $\underset{\sim}{W}$ above where

$$S_k = e^{ju(2k-K-1)} \tag{59}$$

Using $\underset{\sim}{S}$ and $\underset{\sim}{W}$ the quiescent pattern can be described as

$$G_q(\theta) = \underset{\sim}{S}^T \underset{\sim}{W}_q = \sum_{k=1}^{K} e^{j(u-u_0)(2k-K-1)} \tag{60}$$

Similarly, $B_k^* = b_k W_{qk}$ and

$$W_k = B_k^* - V_k \tag{61}$$

It appears that the k-dimensional case is proceeding exactly as the single dimensional case of the previous section. The only difference is that a solution involves a set of K simultaneous differential equations. Starting with Eqs(27) and(28),

$$\tau_o \frac{dV_k}{dt} + V_k = \left(\overline{E_k^* \sum_{i=1}^{k} W_i E_i}\right) \tag{62}$$

Since

$$\frac{dW_k}{dt} = -\frac{dV_k}{dt} \tag{63}$$

it is possible to write in matrix form

$$\tau_o \frac{d\underset{\sim}{W}}{dt} + \underset{\sim}{W} = \underset{\sim}{B}^* - \left[\overline{\underset{\sim}{E}^* \underset{\sim}{W}^T \underset{\sim}{E}}\right]$$

$$= \underset{\sim}{B}^* - \left[\overline{\underset{\sim}{E}^* \underset{\sim}{E}^T}\right] \underset{\sim}{W} \tag{64}$$

The product of $\underset{\sim}{E}^* \underset{\sim}{E}^T$, time averaged, is the cross-correlation matrix of the system inputs. If the inputs are zero mean (few papers explicitly state this) then the matrix is also the covariance matrix. Here it is called $\underset{\sim}{M}$.

$$\underset{\sim}{M} = \left[\overline{\underset{\sim}{E}^* \underset{\sim}{E}^T}\right] = \begin{bmatrix} \overline{E_1^* E_1} & \overline{E_1^* E_2} & \cdots & \overline{E_1^* E_k} \\ \overline{E_2^* E_1} & \overline{E_2^* E_2} & \cdots & \\ \vdots & \vdots & \ddots & \\ \overline{E_k^* E_1} & & & \overline{E_k^* E_k} \end{bmatrix} \tag{65}$$

By evaluating each element, realizing that $\overline{n_i n_k} = 0$ for $i \neq k$,

and assuming independent jammers

$$\underset{\sim}{M} = \underset{\sim}{M}_q + \sum_{i=1}^{I} \underset{\sim}{M}_i \tag{66}$$

$\underset{\sim}{M}_q$ is the diagonal matrix of quiescent noise powers and

$$\underset{\sim}{M}_i = |J_i|^2 \begin{bmatrix} 1 & e^{j2u_i} & e^{j4u_i} \cdots \\ e^{-j2u_i} & 1 & e^{j2u_i} \cdots \\ e^{-j4u_i} & e^{-j2u_i} & 1 \cdots \\ \vdots & \vdots & \vdots \ddots \end{bmatrix} \tag{67}$$

Eq(64) now becomes

$$T_o \frac{d\underset{\sim}{W}}{dt} + \left[\underset{\sim}{I} + \underset{\sim}{M}\right]\underset{\sim}{W} = \underset{\sim}{B}^* \tag{68}$$

where $\underset{\sim}{I}$ is the identity matrix. From Eq(66) and (67) it is clear that $\underset{\sim}{M}$ is a positive-definite, Hermitian matrix. Therefore a solution to Eq(68) can be obtained from an eigensystem of equations when $\underset{\sim}{M}$ is transformed into diagonal form.

Orthogonal System

If λ_i^2 are the eigenvalues and $\hat{e}_i$ the eigenvectors of matrix $\underset{\sim}{M}$ then

$$\left|\underset{\sim}{M} - \lambda_i^2 \underset{\sim}{I}\right|^2 = 0 \quad \text{and} \quad \underset{\sim}{M}\hat{e}_i = \lambda_i^2 \hat{e}_i \tag{69}$$

where

$$\hat{\underset{\sim}{e}}_i^T = \left[e_{i1}, e_{i2}, e_{i3}, \cdots e_{ik} \right] \tag{70}$$

If $\underset{\sim}{Q}$ is the matrix transformation of eigenvectors then to diagonalize $\underset{\sim}{M}$,

$$\left[\underset{\sim}{Q}\, \underset{\sim}{M}\, \underset{\sim}{Q}^T \right] = \left[\lambda_i^2\, \delta_{ij} \right] \tag{71}$$

where δ_{ij} is the Krondecker delta.
When the transformation is complete such that $\hat{\underset{\sim}{E}} = \underset{\sim}{Q}\underset{\sim}{E}$ or

$$\left[\hat{\underset{\sim}{E}}^* \hat{\underset{\sim}{E}}^T \right] = \lambda_i^2\, \delta_{ij} \tag{72}$$

The system of equations has been orthonormalized and all antenna elements and adaptive loops are now independent from one another. The solution of each independent loop equation is now dependent upon the eigenvalues of the matrix transformation. Eq(68) can be reduced to K equations of the form

$$\tau_o \frac{d\hat{W}_k}{dt} + \left(1 + \lambda_k^2 \right) \hat{W}_k = \hat{B}_k^* \tag{73}$$

where the "hat" indicates matrix quantities in the transformed system. Comparing this to the analysis done in the 2-element case and with Eq(72) note

$$\mu_k = \lambda_k^2 \tag{74}$$

With this observation, it is possible to use Eqs(48) through (52) to carry on the analysis. However, it must be remembered that a transformation has occured such that

$$\underset{\sim}{W} = \underset{\sim}{Q}^T \hat{\underset{\sim}{W}} \tag{75}$$

or

$$W_k = \hat{e}_{1k}\hat{W}_1 + \hat{e}_{2k}\hat{W}_2 + \cdots + \hat{e}_{Kk}\hat{W}_K \tag{76}$$

If the interference is switched on at time $t=0$,

$$\hat{W}_k(0) = \hat{W}_{qk} \tag{77}$$

and Eq(48) becomes

$$\hat{W}_k = \hat{W}_{qk} - \left(1 - e^{-\alpha_k t}\right)\left(\frac{\mu_k - \mu_o}{\mu_k + 1}\right)\hat{W}_{qk} \tag{78}$$

where $\mu_0 = \lambda_0^2$, the quiescent eigenvalues.

Signal-to-noise (interference) optimization is accomplished by maximizing the steering vector $\underset{\sim}{B}^*$ to interference ratio (Ref4:58). The results obtained from this are

$$\underset{\sim}{W}_o = \left[\underset{\sim}{M}^{-1}\underset{\sim}{B}^*\right] \tag{79}$$

or

$$\hat{W}_{ok} = \frac{1}{\mu_k} B_k^* \tag{80}$$

Eq(79) is interesting in that the optimum weights can be obtained by inverting the covariance matrix directly. This result is not used unless steady-state conditions prevail to adaption and no transient analysis is required.

Since a transient analysis is the object of this paper it is necessary to generalize Eq(60) to

$$G(\theta,t) = \underset{\sim}{\hat{W}}^T \underset{\sim}{S} = \sum_{i=1}^{K} \hat{W}_i \hat{S}_i \tag{81}$$

where

$$\hat{S}_i = \underset{\sim}{\hat{e}}_i^T \underset{\sim}{S} = \sum_{k=1}^{K} \hat{e}_{ik} S_k \tag{82}$$

Restating Eq(78) to change the subscripts gives

$$\hat{W}_i = \hat{W}_{qi} - \left(1 - e^{-\alpha_i t}\right)\left(\frac{\mu_i - \mu_o}{\mu_i + 1}\right) \hat{W}_{qi} \tag{83}$$

where

$$\hat{W}_{qi} = \underset{\sim}{\hat{e}}_i^{*T} W_q = \sum_{k=1}^{K} \hat{e}_{ik}^* W_{qk} \tag{84}$$

Eq(83) is of the form showing a beam-steering component minus a retrodirective component. If a summation of independent quiescent weights is considered to form the quiescent pattern then

$$G(\Theta,0) = G_{\hat{g}}(\Theta) \tag{85}$$

and Eqs(81) and (83) give

$$G(\Theta,t) = G_{\hat{g}}(\Theta) - \sum_{i=1}^{K}\left(1-e^{-\alpha_i t}\right)\left(\frac{\mu_i-\mu_0}{\mu_i+1}\right)\hat{W}_{\hat{g}i}\,\hat{S}_i \tag{86}$$

where α_i , μ_i , and μ_0 are as previously defined. Two observations are important here. The first is at the retrodirective component consists of a summation of weighted, independent, eigenvector beams which resulted from the transformation. Secondly, the $(\mu_i-\mu_0)$ term is zero for any eigenvectors which are equal to the quiescent eigenvalue. Also recall that the speed at which the array adapts is dependent upon interference power (as reflected in the eigenvalues).

Eq(86) is used to evaluate the antenna pattern at any instant of time. However, no mention has been made thus far concerning the nulling capability of the array. For this reason, the usual tie to SNR is made in the next section.

Adaptive Array Performance

Recall that the interference scenario calls for a step

function input of the sources at time t=0 . Prior to this time, statistically independent receiver noise is n_o in all adaptive loops. Therefore, $\lambda_0^2 = |n_o|^2$. For convenience, since amplifier gains can be set accordingly, set

$$\mu_o = \lambda_o^2 = |n_o|^2 = 1 \tag{87}$$

Receiver noise is also independent of the interference so total output noise is a summation of the loop noise contributions at any time.

$$|N_o(t)|^2 = \sum_{i=1}^{K} |\hat{W}_i \, n_{oi}|^2 \tag{88}$$

where

$$n_{oi} = \hat{\underset{\sim}{e}}_i^T \underset{\sim}{N}$$

From Eq(78) then

$$|N_o(t)|^2 = |n_o|^2 \sum_{i=1}^{K} \left[1 - \left(1 - e^{-\alpha_i t}\right)\left(\frac{\mu_i - \mu_o}{\mu_i + 1}\right)\right]^2 |\hat{W}_{qi}|^2 \tag{90}$$

If $A_i(t)$ is defined as

$$A_i(t) = \left(1 - e^{-\alpha_i t}\right)\left(\frac{\mu_i - \mu_o}{\mu_i + 1}\right) \tag{91}$$

then Eq(89) becomes

$$|N_o(t)|^2 = |n_o|^2 \sum_{i=1}^{K} \left[1 - A_i(t) \right]^2 |\hat{W}_{qi}|^2 \qquad (92)$$

For quiescent conditions at t=0 , $A_i(t)=0$ and

$$|N_o(0)|^2 = |n_o|^2 \sum_{k=1}^{K} |W_{qk}|^2 \qquad (93)$$

Therefore,

$$|N_o(0)|^2 = |n_o|^2 \sum_{k=1}^{K} |W_{qk}|^2 - \sum_{i=1}^{K} \left[2 - A_i(t) \right] A_i t \, |\hat{W}_{qi}|^2 \qquad (94)$$

The noise power from the interference sources is easily seen to be a summation of each power times the power gain at the source azimuth.

$$|J(t)|^2 = |n_o|^2 \sum_{r=1}^{R} P_r \, G^2(\theta_r, t) \qquad (95)$$

where P_r is the rth source power and θ_r is its location. Total output noise (in relation to a desired signal) is a summation of total noise, Eq(94), and interference noise, Eq(95). The increase in total output noise is the ratio of this sum to quiescent noise. This concept is similar to a

S+N/N ratio. In this case a J+N/N ratio is derived. Combining the equations gives

$$\frac{|JN(t)|^2}{|N_o(t)|^2} = 1 + \left[\frac{\sum_{r=1}^{R} P_r G^2(\theta_r, t) - \sum_{i=1}^{K} [2 - A_i(t)] A_i(t) |\hat{W}_{gi}|^2}{\sum_{k=1}^{K} |W_{gk}|^2} \right] \qquad (96)$$

Since the desired signal is assumed to be broadside to the array ($\theta_s = 0^0$) , Eq(57) reduces the denominator above to K. By normalizing Eq(96) with respect to the desired signal a degradation ratio results where

$$D = \left[\frac{G_g(\theta_s)}{G^2(\theta_s, t)} \right] \left[\frac{|JN(t)|^2}{|N_o(t)|^2} \right] \qquad (97)$$

Bandwidth

In the proceeding treatment of adaptive arrays no mention has been made to the interfering signals and their characteristics. In fact, the phase factor u was defined in Eq(3) to represent a true time-delay relationship between elements. A realistic interference source will not consist of a CW signal; it will have some bandwidth. All previous analysis implicitly assumed an interference source consisting of a single spectral line at f_0 , the RF carrier frequency. This section will incorporate bandwidth into the

adaptive array model.

Recall Eq(3), the phase factor

$$u_i = \frac{\pi d}{\lambda} \sin \theta_i \qquad (98)$$

for each interference source. If a half-wavelength (with respect to f_0) element spacing is assumed then

$$u_i = \frac{f}{f_0} \frac{\pi}{2} \sin \theta_i \qquad (99)$$

where f is the interfering spectral line. Although the model will not allow the incorporation of a continuous power spectral density, it is possible to approximate a flat density with many discrete spectral lines. It is also possible to have the interference bandwidth lie anywhere in the RF bandwidth. For a narrowband system the usual convention is that the RF bandwidth be less than 10 percent of the RF center frequency. Therefore the frequency ratio above is bounded by

$$.95 \leq \frac{f}{f_0} \leq 1.05 \qquad (100)$$

It is also possible to define f as

$$f = f_0 + \Delta f + \Delta f_l \qquad (101)$$

where Δf is the difference in frequency between f_0 and f, the center of the interference spectrum. Δf_l is the difference between f and the lth spectral line interference. Figure 6 shows these relationships. In this analysis it must be

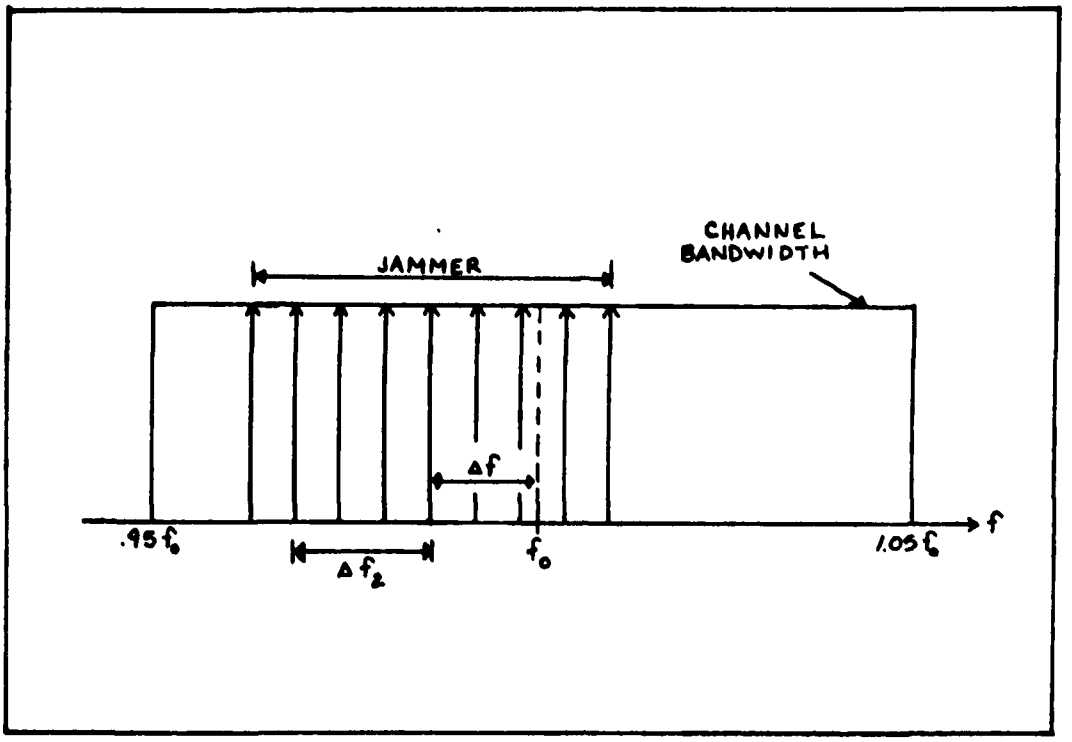

Figure 6 Interference with Bandwidth

assumed that the discrete lines are independent. For RF signals, the cross-correlation over many cycles will be zero.

Eq(98) can be rewritten as

$$u_{rl} = \frac{f_0 + (f - f_0) + \Delta f_l}{f_0} \frac{\pi}{2} \sin \theta_r$$

$$= \frac{f + \Delta f_l}{f_0} \frac{\pi}{2} \sin \theta_r \qquad (102)$$

where the notation rl refers to the rth interference source, lth spectral line. If $f=f_0$ then the maximum Δf_l is $\pm .05$ and it is possible to relate the source bandwidth B_r, the number of spectral lines L_r, and the lth line as

$$\frac{\Delta f_\ell}{f_o} = \frac{.1\,B_r}{100}\left[-\frac{1}{2} + \left(\frac{\ell - 1}{L_r - 1}\right)\right] \qquad (103)$$

Eq(102) then becomes

$$u_{r\ell} = \left[\frac{f}{f_o} + .1\,B_r\left(-\frac{1}{2} + \left(\frac{\ell - 1}{L_r - 1}\right)\right)\right]\frac{\pi}{2}\,\sin\theta_r \qquad (104)$$

where B_r is expressed as a ratio of jammer bandwidth to RF bandwidth.

The question now evident is the number of spectral lines needed to approximate the flat spectrum of the interference source. An answer to this is found in the concept of time-bandwidth product (Ref 9). When investigating orthogonal signalling rates or the number of orthogonal functions required to approximate an ideal bandpass system at 90% power level the following holds

$$N = 2.4WT \qquad (105)$$

In this equation, N is the number of orthogonal signals, W the bandwidth, and T the time interval (signalling time). By assuming that the interfering spectral lines are independent the above can be used to indicate a number for L_r. L_r can be approximated by saying that T is the time required to estimate the covariance. For example, if τ_0 is one microsecond, and $5\tau_0$ is required for an estimate then

13 lines would approximate a continuous spectrum 1MHz wide.

Since the interference signal now has bandwidth it is necessary to redefine the covariance matrix $\underset{\sim}{M}$. If $\underset{\sim}{M}_q$ is the identity matrix (for computational ease)

$$\underset{\sim}{M} = \underset{\sim}{I} + \sum_{r=1}^{R} \sum_{\ell=1}^{L_r} P_{r\ell}\, \underset{\sim}{M}_{r\ell} \tag{106}$$

where

$$\underset{\sim}{M}_{r\ell} = \left[\underset{\sim}{S}^{*}_{r\ell}\, \underset{\sim}{S}^{T}_{r\ell}\right] \tag{107}$$

$$S_{r\ell k} = e^{\,j u_{r\ell}(2k-K-1)} \tag{108}$$

$$P_{r\ell} = \frac{P_r}{L_r} \tag{109}$$

S_k has been redefined so changes must be made to any affected previous equations. Eq(86), if used to evaluate the antenna pattern only, does not require any changes for the following reasons. Recall that $\underset{\sim}{M}$ was formed by summing the source vectors for each interfering spectral line. Once this is accomplished, the eigenvectors and eigenvectors are calculated. These represent transformed weights of which only K exist, so at any instant of time, $\hat{W}_k$ assumes one value. $\hat{W}_k$ can therefore only influence one degree of freedom in the retrodirective beam, and Eq(82), used in Eq(86), should not be

changed. In this case S_k represents a far field angle variable only.

On the other hand, Eq(96), does require some modification to include bandwidth. It can be shown (Ref4:35-39) that spectral lines at f_0 are nulled the most. The farther each spectral line is away form f_0, the less it is nulled. If an interference source were not centered on f, then an adaption to the spectrum center would not occur. When calculating the increase in total output noise power, these observations require some consideration. The weight, $\hat{W}_k$, forming a component of the retrodirective beam will not cancel each interfering spectral line equally as noted above since it can only assume one amplitude and phase value. The interference is composed of many phase values. To accurately determine the total output noise power, the eigenvector and eigenvalue of the kth loop must be applied to each spectral line in the interfering source. To reflect the above information the noise contribution of the interfering sources, Eq(95), requires changes. After redefining S_k with Eq(108), $\hat{S}_i$ now becomes

$$\hat{S}_{rli} = \sum_{k=1}^{K} \hat{e}_{ik} S_{rlk} \qquad (110)$$

With this substitution $G^2(\theta_r,t)$ for each spectral line can be evaluated. The total interference noise power must then

be renormalized to account for L_r lines so

$$|J(t)|^2 = |n_o|^2 \sum_{r=1}^{R} \sum_{l=1}^{L_r} P_{rl}\, G_{rl}^2(\Theta_r, t) \qquad (111)$$

Eq(96) then becomes

$$\frac{|JN(t)|^2}{|N_o(t)|^2} = 1 + \left[\frac{\sum_{r=1}^{R} \sum_{l=1}^{L_r} P_{rl}\, G_{rl}^2(\Theta, t) - \sum_{i=1}^{K} [2 - A_i(t)]\, A_i(t) |\hat{W}_{gi}|^2}{K} \right] \qquad (112)$$

for a broadside array.

This concludes the section on the adaptive array model. Many equations have been given to understand Gabriel's array algorithm, most of which only aid the derivation. However, Eq(86) specifying the array pattern, and Eq(97) specifying the transient degradation are important. Both have decaying exponential terms which could be affected by an AGC. The time constants are power dependent and any transient AGC response would make them time dependent also.

III. Automatic Gain Control Model

The choice of an AGC model to be used in conjunction with the adaptive array model is difficult, due to the non-linear nature of AGC circuits. Since Oliver (Ref 10) in 1948 most work has keyed upon feedback type analysis to obtain static or small signal perturbation solutions to non-linear systems employing various gain characteristics. Of note, in addition to Oliver, are Victor and Brockman (Ref 11), Banta (Ref 12), Plotkin (Ref 13), Gill and Leong (Ref 14), and recently, Ohlson (Ref 15).

Generalized Model

Without prior information, an intuitive approach to controlling the level of a continuous signal would be to take a short-time average. This average, could then be used to control an amplifier with some desired gain characteristic. Historically, this has been the case with one minor change; the use of a low-pass filter (or integrator) to obtain the level information. For this analysis, following Ohlson, the low-pass filter has been approximated by an integrator. Figure 7 represents a generalized model typically used by the individuals noted above. Shown as a gain characteristic is the function used in this analysis. Other gain characteristics have been used but this one (Ref 7) has been approximated in most modern receiver designs.

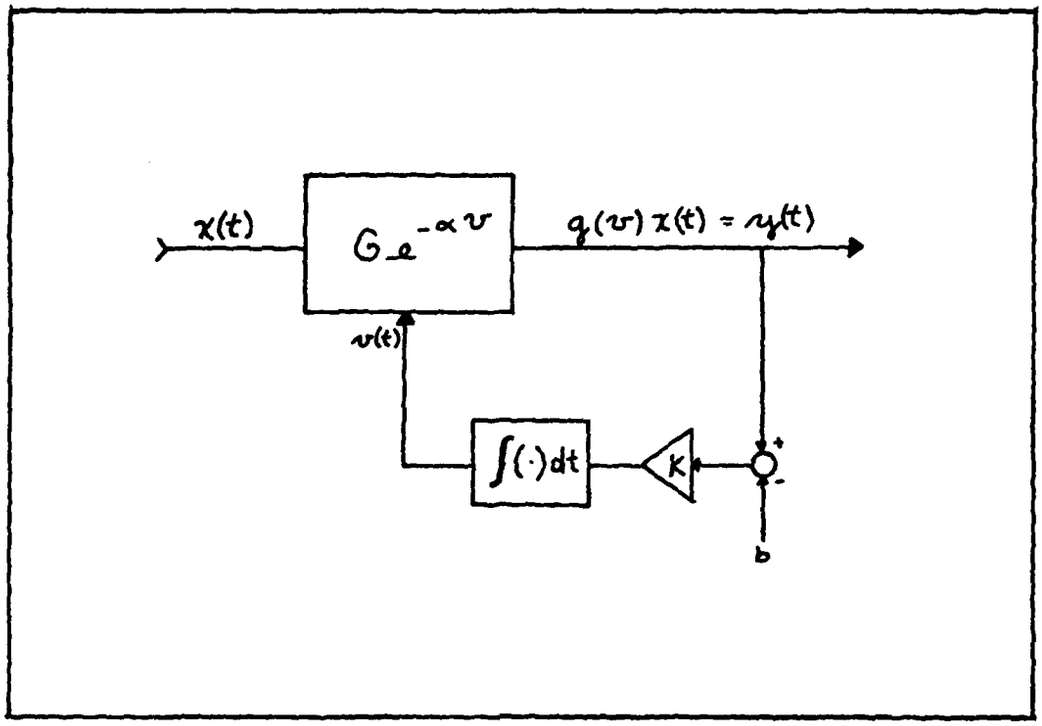

Figure 7 Generalized AGC loop

Model Analysis

Since Ohlson's results have linearized the above model for a broader case than either the small signal variation or static analysis, it is used here to gain insight into AGC operation and modeling. The gain characteristic is

$$q(v) = G e^{-\alpha v} \tag{113}$$

where time t is implicit in v . The differential equation describing the feedback loop is

$$\dot{v} = K(y - b) = K(xG e^{-\alpha v} - b) \tag{114}$$

From Eq(113) it is seen that

$$\dot{g} = -\alpha g \dot{v} \tag{115}$$

so Eq(114) becomes

$$\dot{g} + K\alpha x g^2 - K\alpha b g = 0 \tag{116}$$

To solve this differential equation a substitution $z=g^2$ is made to convert to a first-order linear differential equation. By solving and returning to g by the inverse substitution, gives

$$g(v(t)) = \left[\frac{e^{-t/\tau}}{g(v_0)} + \frac{1}{b} \int_0^t \frac{1}{\tau} e^{-(t-U)/\tau} x(U)\, dU \right]^{-1} \tag{117}$$

where

$$\tau = \frac{1}{K\alpha b} \quad \text{and} \quad v_0 = v(0) \tag{118}$$

Recognizing that the integral above is a convolution of $h(t)*x(t)$ where

$$h(t) = \begin{cases} \frac{1}{\tau} e^{-t/\tau} & t \geq 0 \\ 0 & t < 0 \end{cases} \tag{119}$$

The results in Eqs(117) and (119) are pleasing because the voltage-controlled attenuation of x(t) is a linear function

and because h(t) is a simple RC low pass filter. By combining Eqs(113), (117) and (119),

$$g(v(t)) = \left[\frac{e^{\alpha v_o - \frac{t}{\tau}}}{G} + \frac{1}{b}\left(h(t) * x(t)\right)\right]^{-1} \tag{120}$$

and thus the output, y(t), is

$$y(t) = \frac{x(t)}{\frac{e^{\alpha v_o - \frac{t}{\tau}}}{G} + \frac{1}{b}\left(h(t) * x(t)\right)} \tag{121}$$

At steady-state this becomes

$$y(t) = \frac{b x(t)}{h(t) * x(t)} \tag{122}$$

When investigating a linearization of Eq(122) Ohlson showed that valid linear results were obtained in the case of sinusoids if $h(t)*\Delta x(t) \ll 1$. To see this evaluate Eq (121) for a finite set of sinusoids such that

$$x(t) = \sum_{i=1}^{N} A_i \cos \omega_i t \tag{123}$$

The calculations are laborious, but the result is extremely interesting. It is stated as

$$y(t) = \frac{\sum_{i=1}^{N} A_i \cos \omega_i t}{\left(\frac{1}{b}\sum_{i=1}^{N} A_i K_i \cos(\omega_i t + \Phi_i)\right) + e^{-t/\tau}\left(e^{KV_0} - C\right)} \qquad (124)$$

where

$$C = \frac{1}{b}\sum_{i=1}^{N} A_i K_i \cos \Phi_i \qquad (125)$$

$$K_i = \frac{1}{\sqrt{1+(\omega_i \tau)^2}} \qquad (126)$$

and

$$\Phi_i = -\arctan(\omega_i \tau) \qquad (127)$$

According to Ohlson, a valid linear model would than require $A_i K_i << 1$. This condition is much weaker than those of small signal or static analysis. However, Ohlson has incorrectly generalized to what appears to be a weaker linearization condition. He has stated that linearization is valid if the small signal variation or $h(t)*\Delta x(t)<<1$ condition is met. His generalization is erroneous because his condition is a subset of the small signal variation case. This observation requires that the small signal variation and convolution conditions be met simultaneously. Returning to Eq(124) it is

seen that if $\omega\tau >> 1$ then $K_i \simeq 0$ and if $\omega\tau << 1$ then $K_i \simeq 1$. Because there are no set limits for the small signal variation case Ohlson's AGC model is still useful. His results give an indication of when those limits are exceeded regardless of the amount of signal variation. In other words, the convolution condition will tell when the small signal variation condition is no longer valid.

Linear model

Ohlson's model is not easily implemented during a simulation of AGC action. For this reason it is desirable to insure a linear case. To accomplish this expand the exponential form of $g(v(t))$ in a series and truncate all non-linear terms. This can be done by expanding the original exponential gain function as

$$g(v(t)) = 1 - \alpha v(t) + \alpha^2 v^2(t) - + - \ldots \qquad (128)$$

If all non-linear terms are truncated this equation becomes

$$g(v(t)) = 1 - \alpha v(t) \qquad (129)$$

The amplifier/integrator can be modelled as a simple low-pass RC filter with Laplace transfer function

$$F(s) = \frac{1}{s+\beta} \qquad (130)$$

The two equations which specify the loop behavior then become

$$y(t) = x(t)\left[1 - \alpha v(t)\right] \tag{131}$$

and

$$v(t) = f(t) * \left[y(t) - b\right] \tag{132}$$

If x(t) is defined to be a constant K , then the corresponding Laplace domain equations become

$$Y(s) = \frac{K}{s} - K\alpha V(s) \tag{133}$$

and

$$V(s) = F(s)Y(s) - \frac{b}{s}F(s) \tag{134}$$

Solving Eq(133) and Eq(134) gives

$$Y(s) = \frac{K(1 + \alpha b F(s))}{s(1 + K\alpha F(s))} \tag{135}$$

Substituting in Eq(130) and taking the inverse Laplace transform gives

$$y(t) = \frac{K}{K\alpha + \beta}\left[(\beta + \alpha b)\,u(t) + \alpha(K - b)e^{-(K\alpha + \beta)t}\right] \tag{136}$$

Eq (136) gives the AGC output as a function of time for a constant unit step input. This model makes intuitive sense because

$$r_y(0) = K \tag{137}$$

and

$$r_y(\infty) = \frac{K(\beta + \alpha b)}{K\alpha + \beta} \tag{138}$$

For realistic implementation the bandwidth of the filter should be much less than the closed loop bandwidth. In addition, the steady-state output should be close to the bias b. For the extreme case where the filter is a perfect integrator ($\beta=0$) the steady state output is identically the bias. For purposes of this thesis

$$\beta << K\alpha \tag{139}$$

with the additional constraint that

$$r_y(\infty) \approx b \tag{140}$$

This again makes intuitive sense for if the filter bandwidth becomes equal to the closed cloop AGC bandwidth then no averaging has taken place and no signal attenuation (or gain) results.

AGC Placement and Expected Results

AGC circuitry can be placed in one of several locations within the adaptive array. Possible locations include the RF section, IF section, or even within the signal branches of the adaptive circuitry. Gabriel has placed a hard limiter in the conjugate signal branch of each adaptive loop. This placement requires extensive modification of the adaptive loop equations and does not protect the signal/weight correlation mixer from high levels. AGC placement in the IF section does protect this mixer and has the additional advantage of fitting in with the signal envelope analysis done in Section III. The jammer power then is the quantity which is controlled by the AGC circuitry.

The addition of the AGC circuitry prior to the actual adaptive loops means that the power and hence the eigenvalue of each loop is affected. Recall the exponential terms in Eq(83) (and others) whose decay is dependent upon α_i where

$$\alpha_i = \frac{\lambda_i^2 + 1}{T_0} \tag{141}$$

Eq(83) also contained the term

$$\frac{\lambda_i^2 - 1}{\lambda_i^2 + 1}$$

For large eigenvalues this is close to unity and will not be included in the following analysis. Returning to the exponential and substituting a normalized Eq(136) to reflect time-

varying eigenvalues gives

$$e^{-\left[\frac{\lambda_i^2}{C_1}\left(C_2 + C_3 e^{-C_1 t}\right) + 1\right]\frac{t}{\tau_0}} \tag{142}$$

The constants K , α , β , and b have been combined into the C constants and are grouped exactly as in Eq(136). The derivative of this term is

$$\frac{d}{dt}\left(e^{x(t)}\right) = e^{x(t)}\frac{d\,x(t)}{dt} \tag{143}$$

In solving for the maxima and minima of Eq(142), Eq(143) is set equal to zero. Clearly, the value(s) of t for which the derivative of the time-varying exponent, x(t) , is zero yields the same result. This derivative is,

$$\left(\frac{\lambda_i^2 C_2}{C_1} + 1\right) + \left(1 - C_1(t)\right)\left(\frac{\lambda_i^2 C_3}{C_1}\right) e^{-C_1 t} \tag{144}$$

If the relative maximum at t=0 and relative minimum at infinity are neglected, there could exist other maxima and minima on the open interval $(0,\infty)$. The existance of these points is not guaranteed for all real constant. However, their existence at all is significant.

The above analysis suggests that there exist values for K , α , β , and b which change the strictly monotonically decreasing nature of Eq(83). Specifically, the

adaptive weight will, on some interval, exhibit an increase in magnitude. This increase must be mirrored in some manner in the antenna pattern and signal degradation, Eqs(86) and (97) respectively. The zeros of Eq(144) could be obtained by numerical methods. This shall not be accomplished directly, for the transient SNR degradation curve will give the same information. A simulation of the AGC/array model algorithm whose output is a plot of the transient SNR degradation is the subject of the next section.

IV. Simulation

Program Overview

The equations which specify the AGC/array algorithm were simulated for a three-element array. Output consisted of antenna pattern and transient SNR degradation plots. The computer program was coded to simulate the algorithm as defined in Eqs(86) and (112). Auxillary equations which were used are Eq(52), (74), (87), (104), (106), and (109). The AGC was incorporated using Eq(136) and was applied directly to jammer power. Following Gabriel, the dynamic range of each correlator input was 40dB and the adaptive loop time constant, τ_0, was fixed at 12,750 microseconds.

All power levels are referenced to a 1 Watt (0 dBW) noise floor for convenience. Since the dynamic range of any signal branch was limited to 40dB, the AGC bias, b, was chosen at 30dB. The AGC feedback filter parameter, β, was set at 100 to reflect a narrower bandwidth than the overall AGC circuit. Array variables which could be changed were jammer power, center frequency, and bandwidth. In all cases the jammer azimuth was held at 30 degrees. The single AGC parameter which could be varied was α, a design parameter. The decay constant in the AGC ($K\alpha+\beta$) is dependent upon the input power (K in Eq(136)) as well as α. Because α is a design parameter and is an indication of the AGC decay rate it is

subsequently referred to as the AGC time constant.

The legend blocks of the computer generated plots contain information on the jammer scenario. Pattern and SNR degradation plots contain jammer power, azimuth, percent of channel bandwidth (for broadband), and the frequency ratio defining the jammer location within the channel (Eq(100)). Each item is separated by a slash. Antenna pattern plots have additional information on the depth of the null at the jammer azimuth. The "AGC TC" on the degradation curves refers to α . Figure 8 is the quiescent antenna pattern for the 3-element, broadside, adaptive array.

Simulation Results

Table I shows the simulations for which only power or AGC time constant was varied. The AGC time constant α was chosen for cases 3 through 8 so that the total AGC decay constant $(K\alpha+\beta)$ would be equal to or an order of magnitude greater than the steady state decay constant of the adaptive array (approx. 235,000). At the outset it must be explained that no hard performance criteria were applied to the results. Instead, the trends associated with each case were compared and contrasted. However, it must be remembered that the curves do represent transient performance whether depth of the null or steady-state degradation is the measure.

Cases 1 and 2 represent adaptive array performance without an AGC. Inspection of their degradation curves shows the

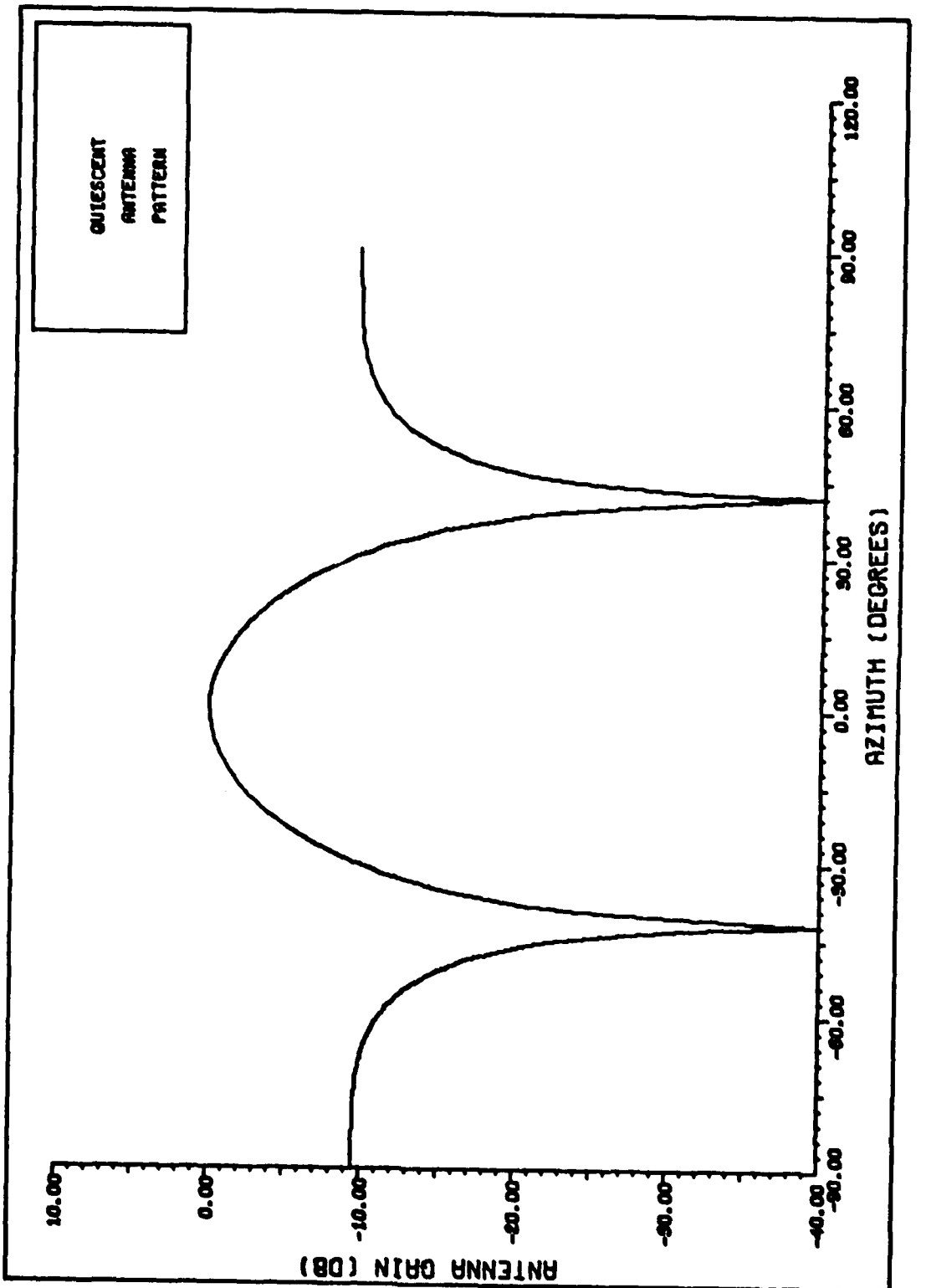

FIGURE 8. QUIESCENT ANTENNA PATTERN

TABLE I

Single Frequency Simulations

Case	Power (dBW)	α	Bandwidth (Percent)	Frequency Ratio
1	30	0	0	1.00
2	40	0	0	1.00
3	50(S)	23.5	0	1.00
4	60(S)	2.35	0	1.00
5	50	2.35	0	1.00
6	60	2.35	0	1.00
7	50	23.5	0	1.00
8	60	23.5	0	1.00

performance to be monotonically decreasing. Cases 3 and 4 shows the effect of an AGC approximately 10 times faster than the adaptive loop for a saturated correlation mixer. The S beside the time constant indicates this in these and following cases. The saturation effect was simulated by limiting the adaptive loop input power to 40dB until the AGC brought the power below that level. Contrasting this with Cases 5 through 8 it can be seen that the unsaturated simulations null the jammer faster initially. This is because the eigenvalues are not constrained. The adaptive loop is nulling the jammer at a fast rate. Because the adapted patterns of Cases 5 through

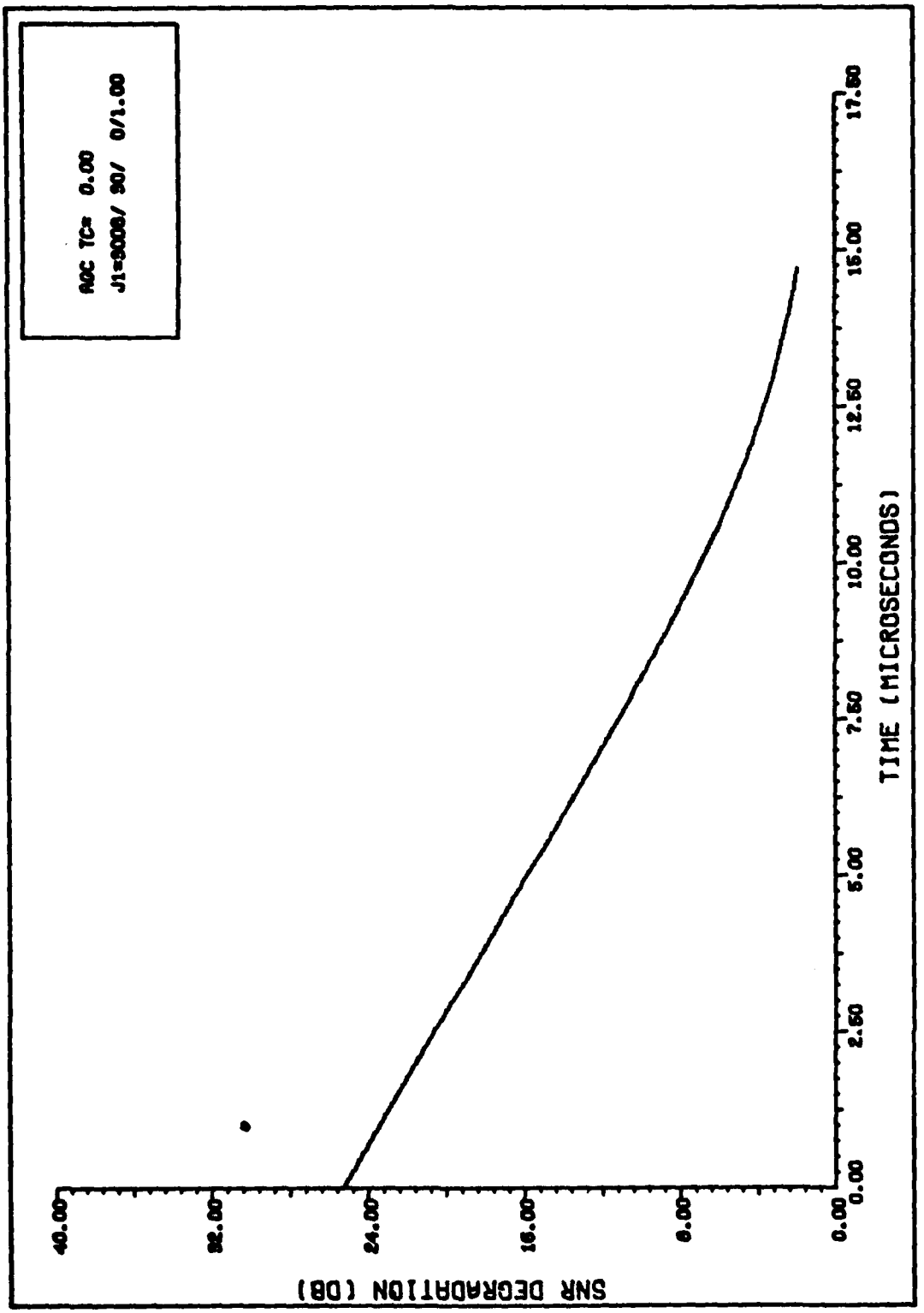

FIGURE 9. TRANSIENT DEGRADATION (CASE 1)

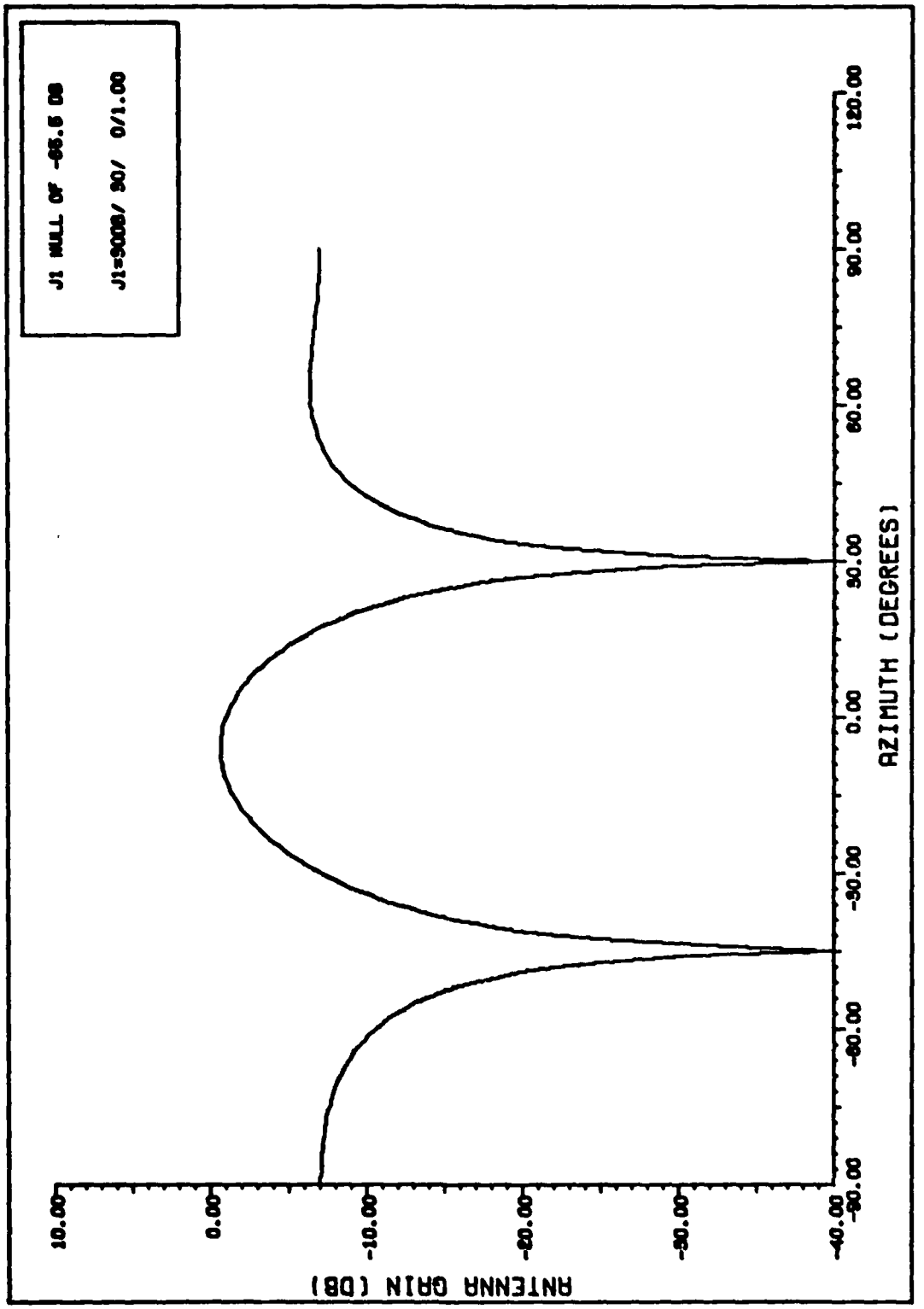

FIGURE 10. ADAPTED ANTENNA PATTERN (CASE 1)

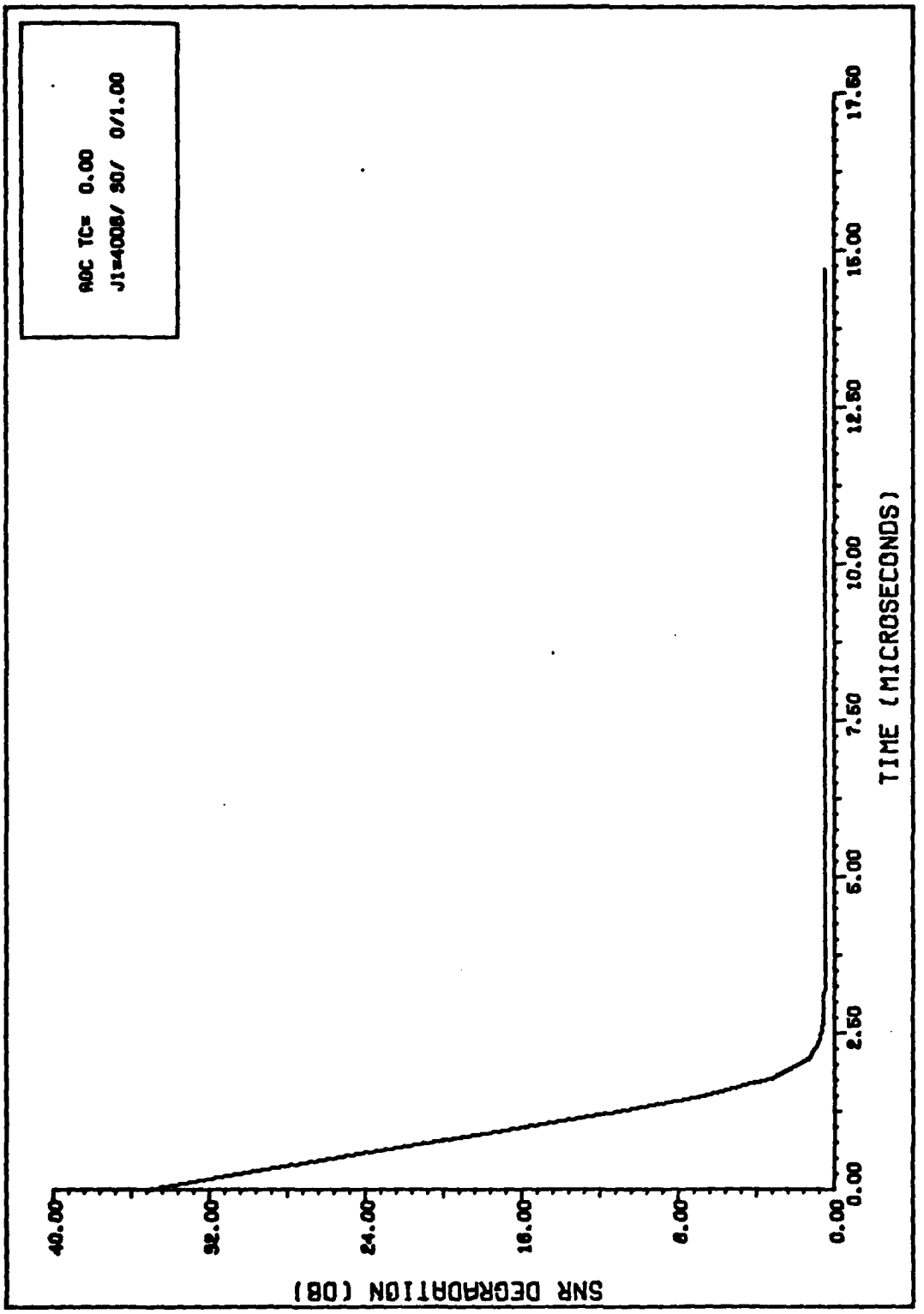

FIGURE 11. TRANSIENT DEGRADATION (CASE 2)

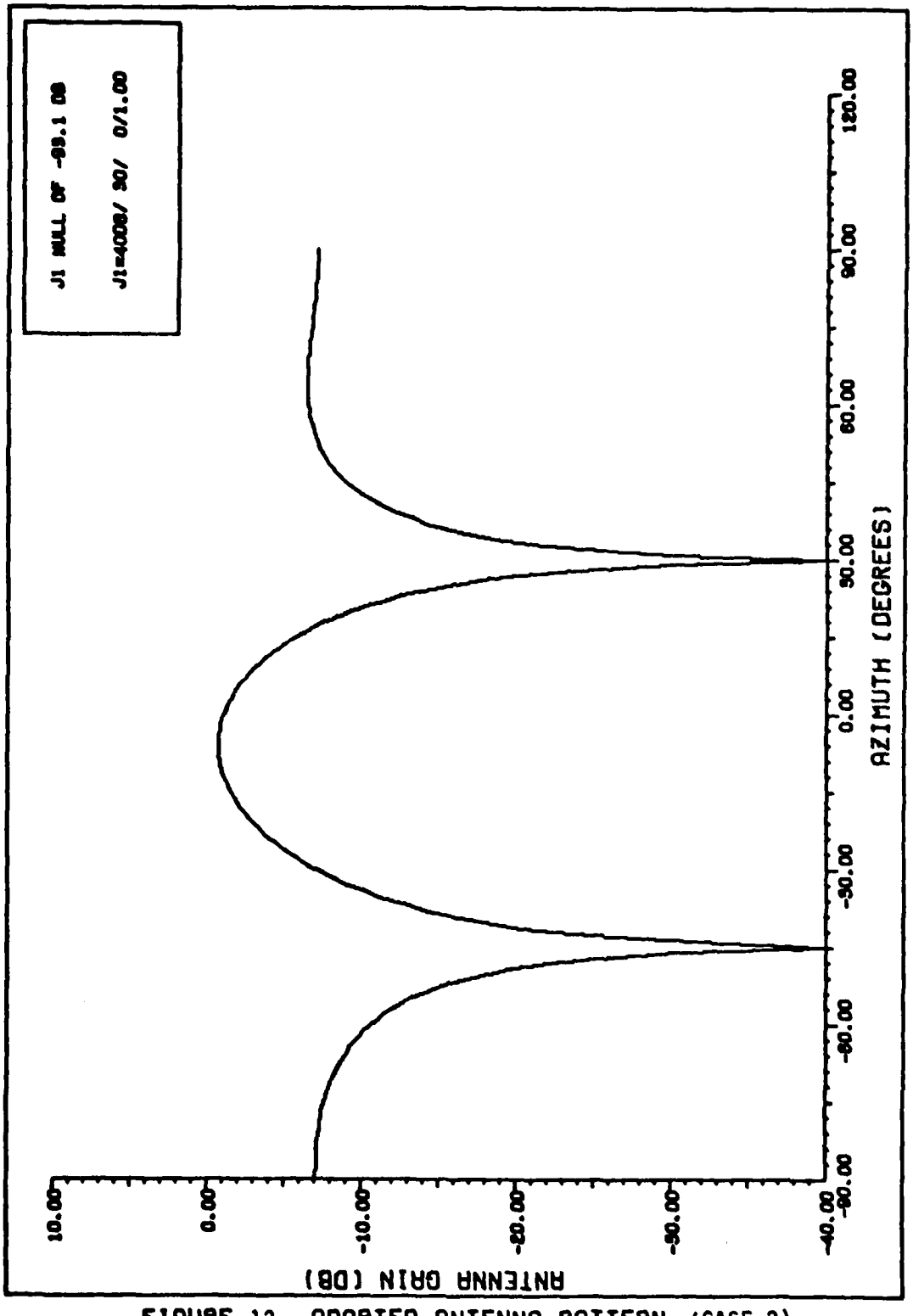

FIGURE 12. ADAPTED ANTENNA PATTERN (CASE 2)

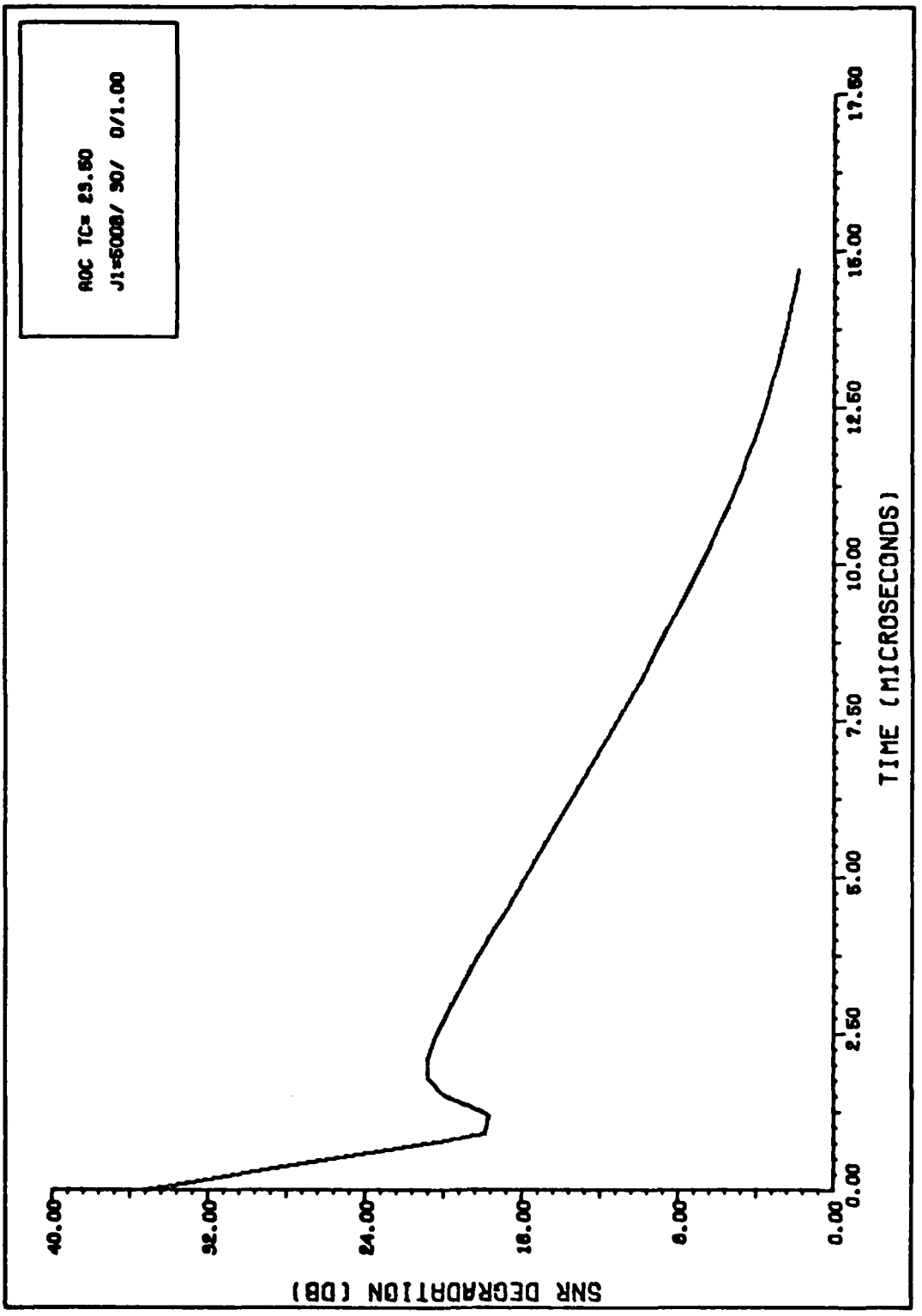

FIGURE 13. TRANSIENT DEGRADATION (CASE 3)

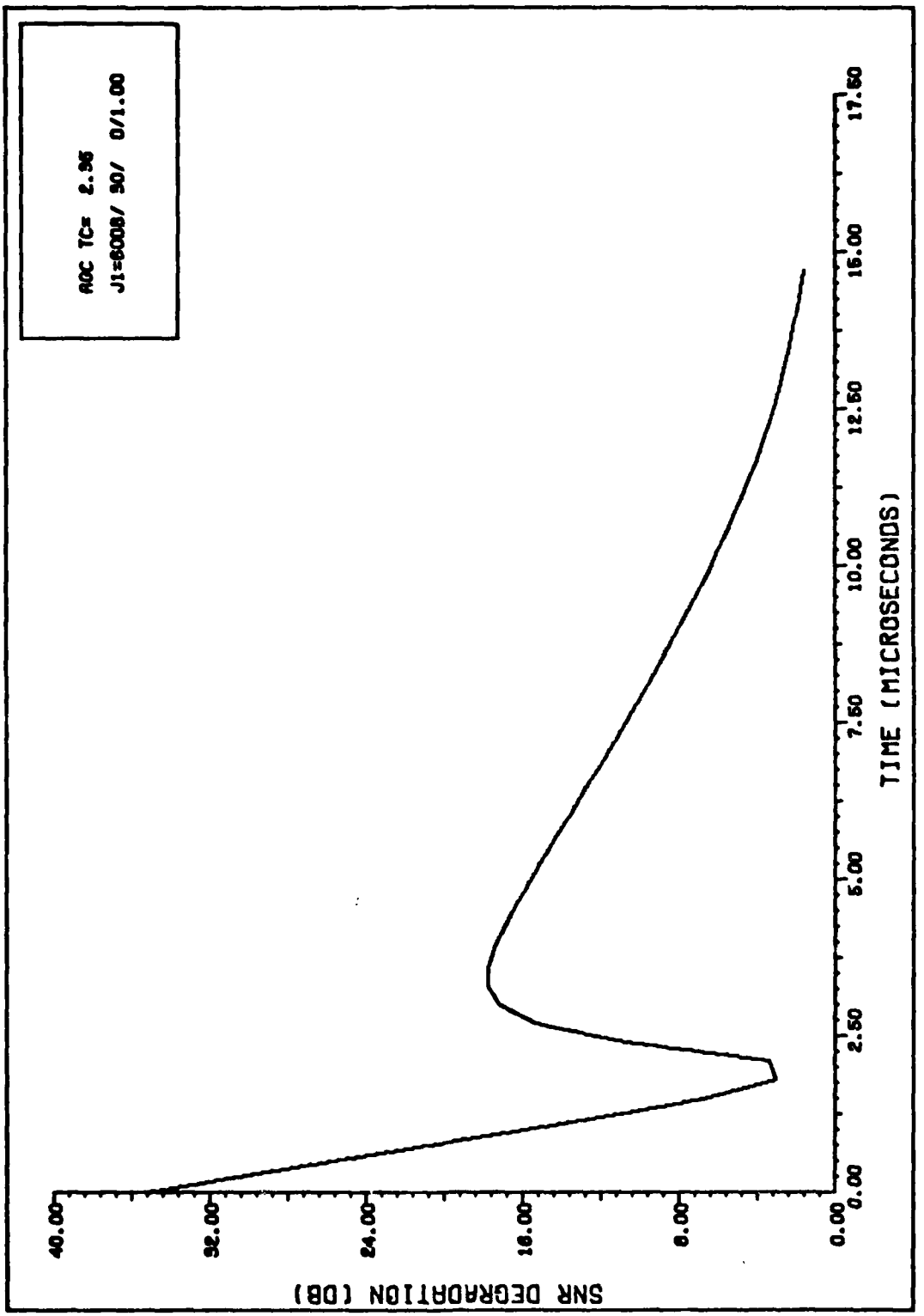

FIGURE 14. TRANSIENT DEGRADATION (CASE 4)

8 are identical (above -40dB) they are not included. Comparing Cases 5 and 7 shows the effect of an increasing AGC time constant. As the AGC becomes faster the initial dip in the degradation curve moves to the right. The increasing degradation then rises and eventually becomes asymptotic to the degradation of case 1. This is to be expected, for the AGC bias has been set to 30dB.

Case 7 also confirms the assertion in the previous section that other relative maxima and minima exist. In fact, the evaluation of Eq(144) for the AGC parameters in Case 7 would yield two times, both of which agree with the degradation curve of case 7.

Table II shows simulations for broadband single jammers. In these cases the time constant was held constant at 5.0 and the bandwidth and frequency ratio varied. For comparison cases 9 through 12 present saturated and unsaturated narrowband simulations. The azimuth is held constant at 30 degrees.

A comparison of cases 12 and 13 shows a large change in transient degradation during periods when the AGC is still transient (not in steady-state). Shown is a comparison between a single spectral line and a bandwidth of 25 percent. Gabriel (Ref4:35-39) has shown that the farther away from center frequency each spectral line is the more it degrades the desired signal. This is expected because the antenna array is designed with element spacing related to channel

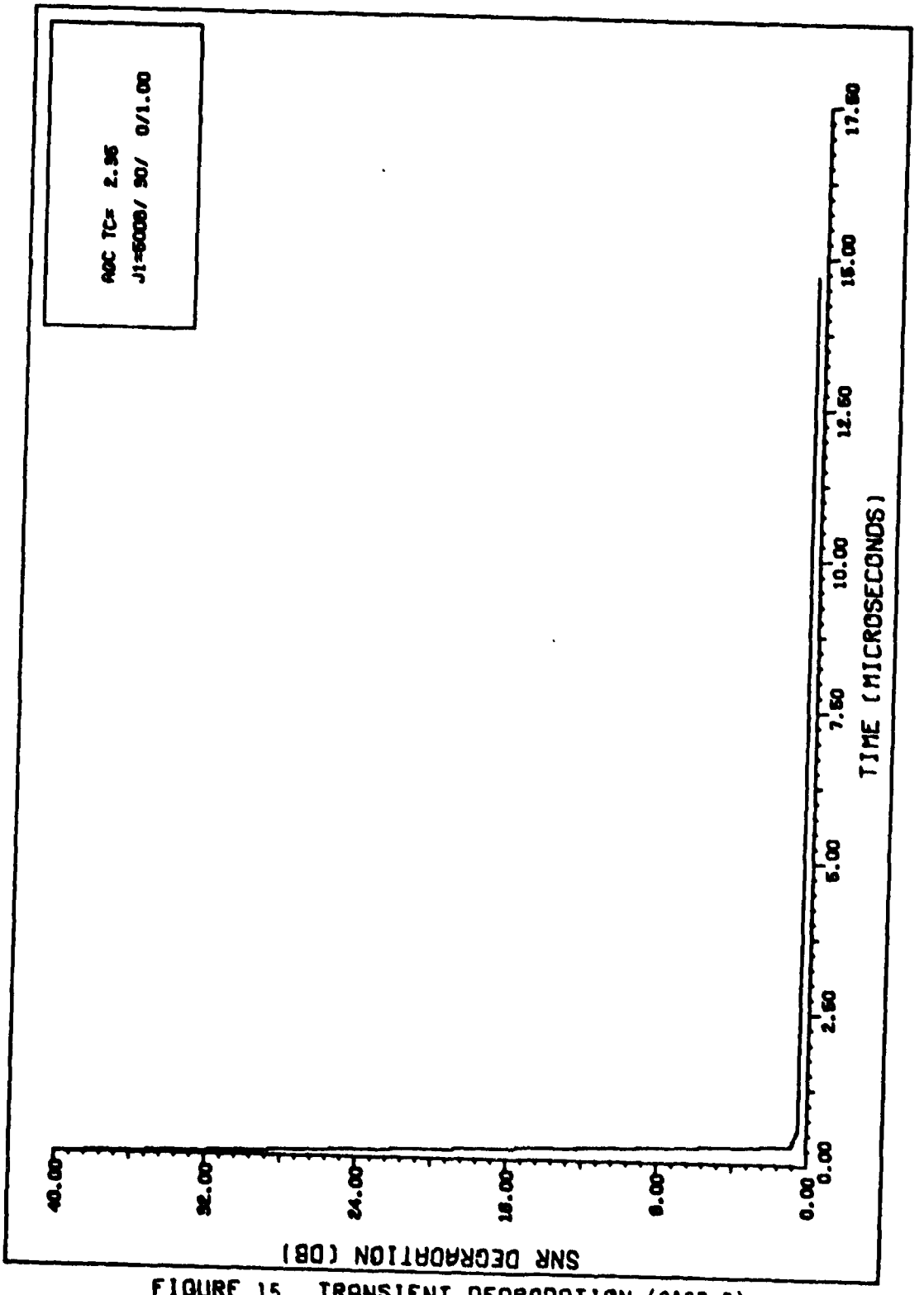

FIGURE 15. TRANSIENT DEGRADATION (CASE 5)

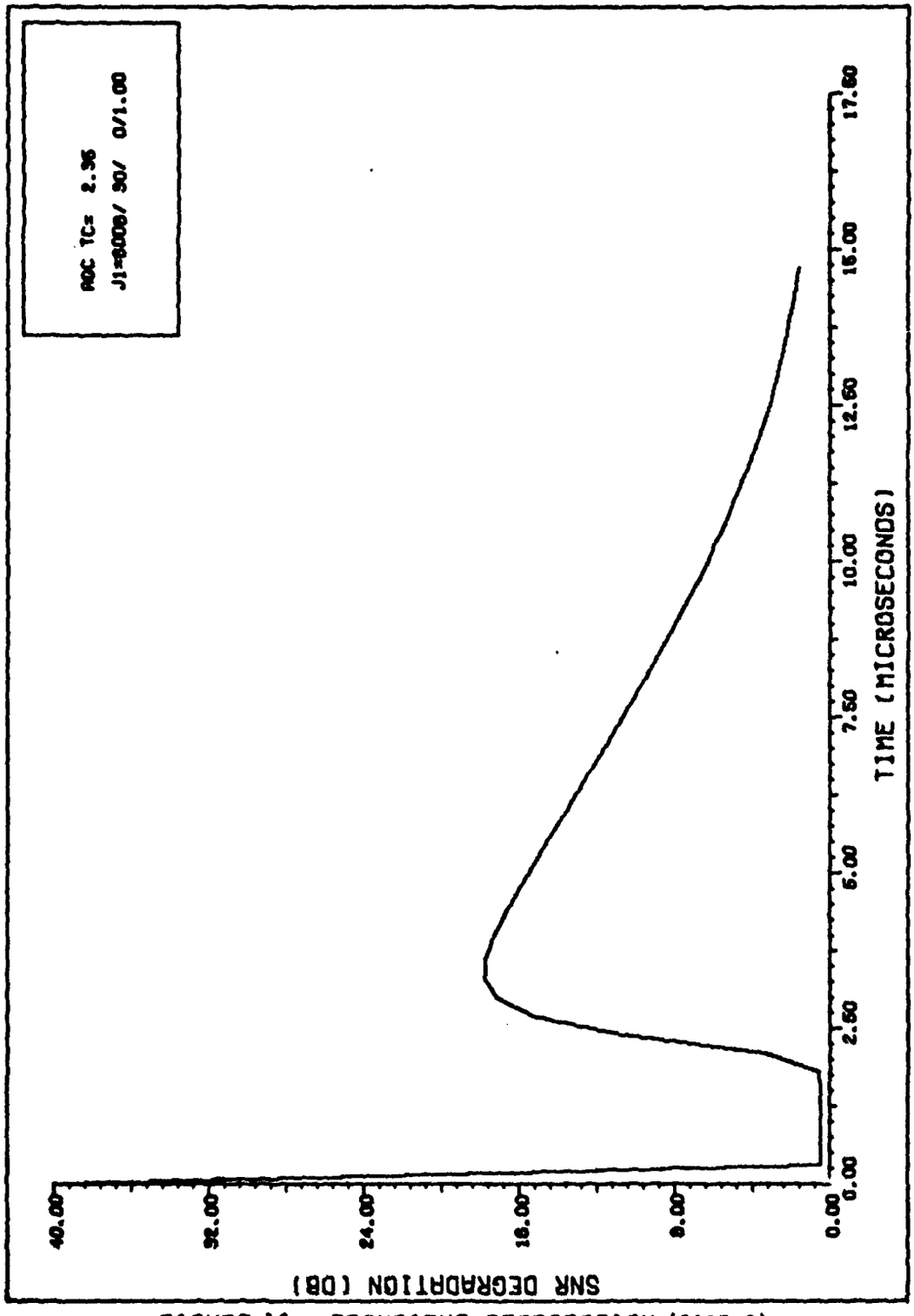

FIGURE 16. TRANSIENT DEGRADATION (CASE 6)

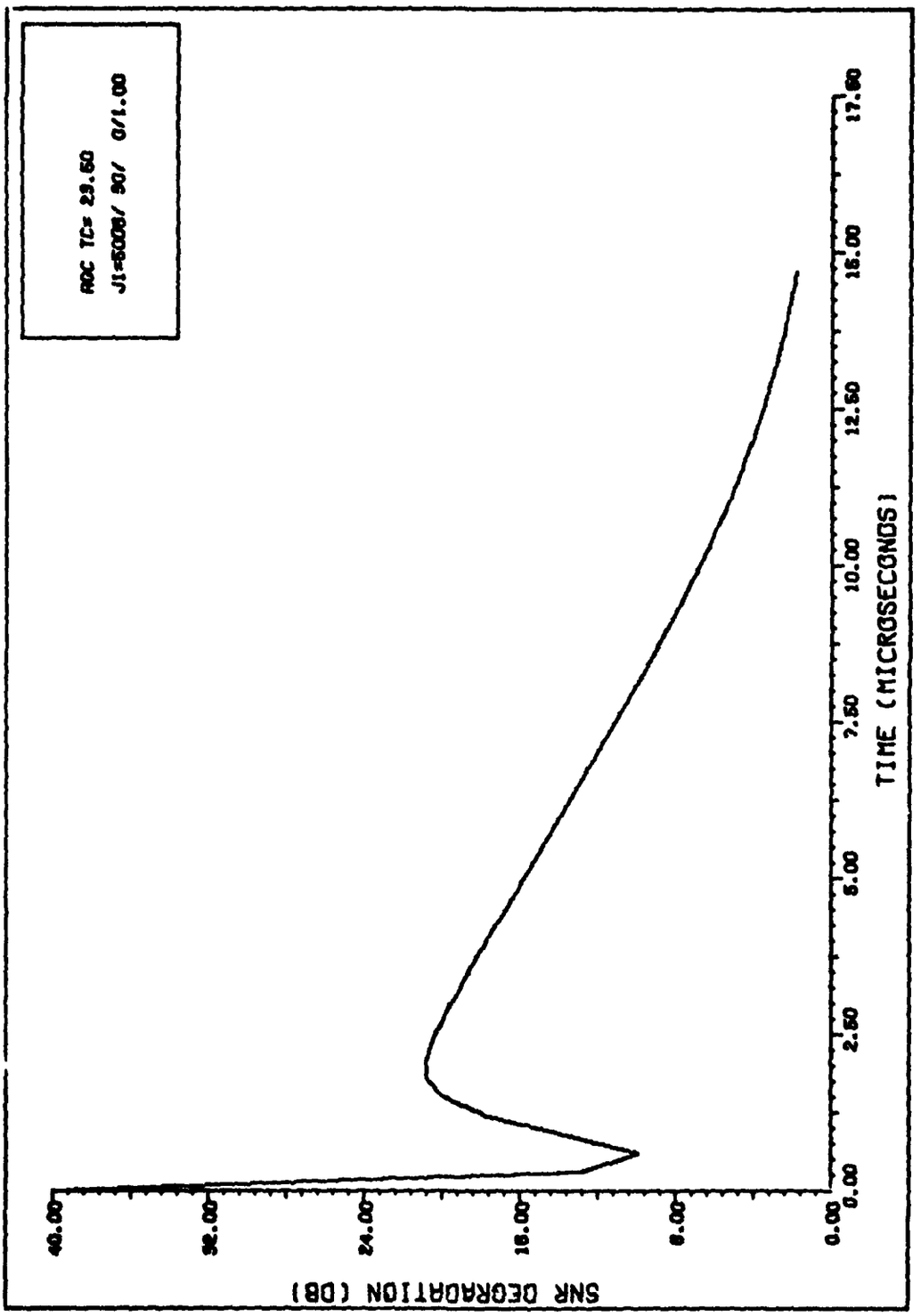

FIGURE 17. TRANSIENT DEGRADATION (CASE 7)

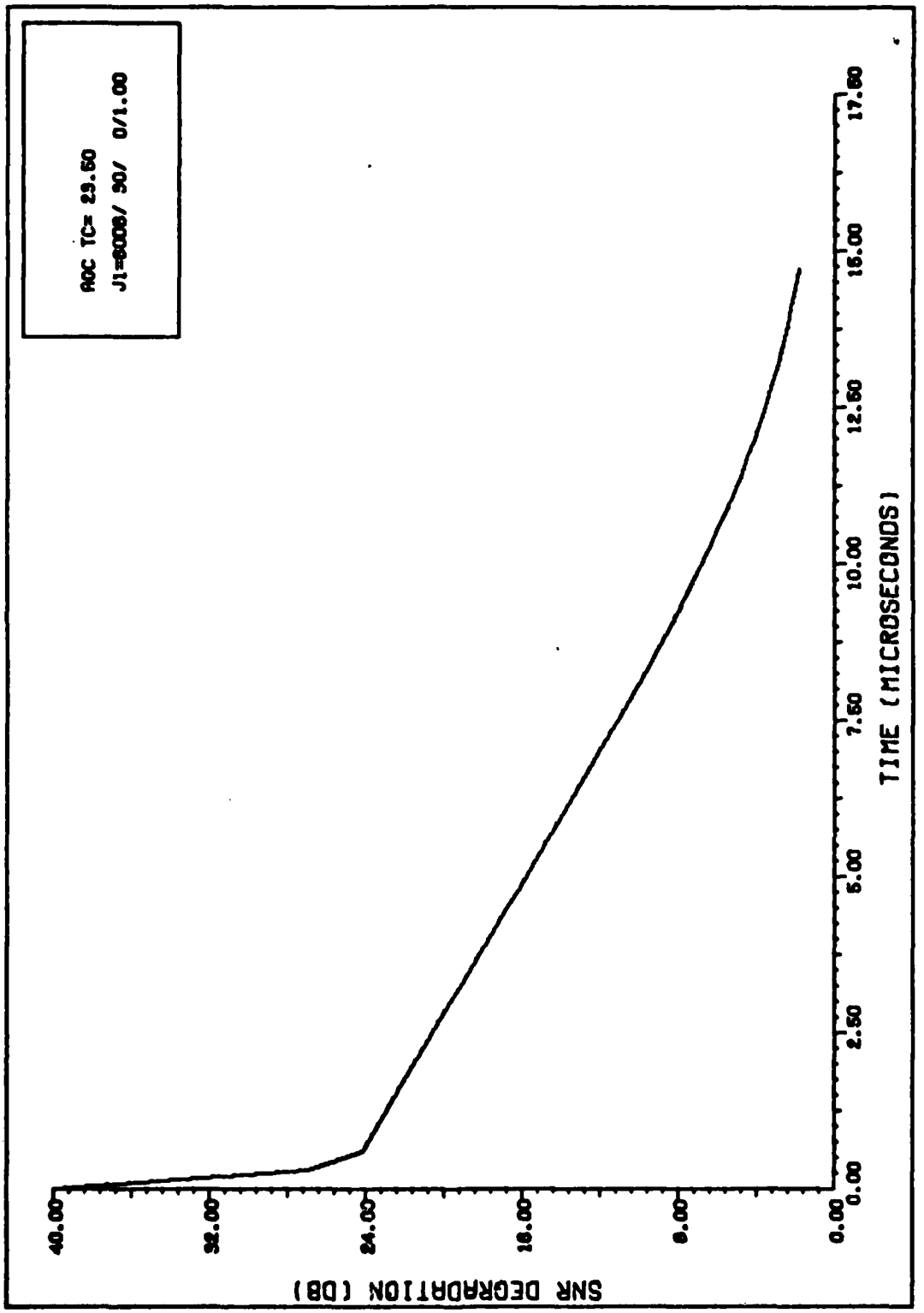

FIGURE 18. TRANSIENT DEGRADATION (CASE 8)

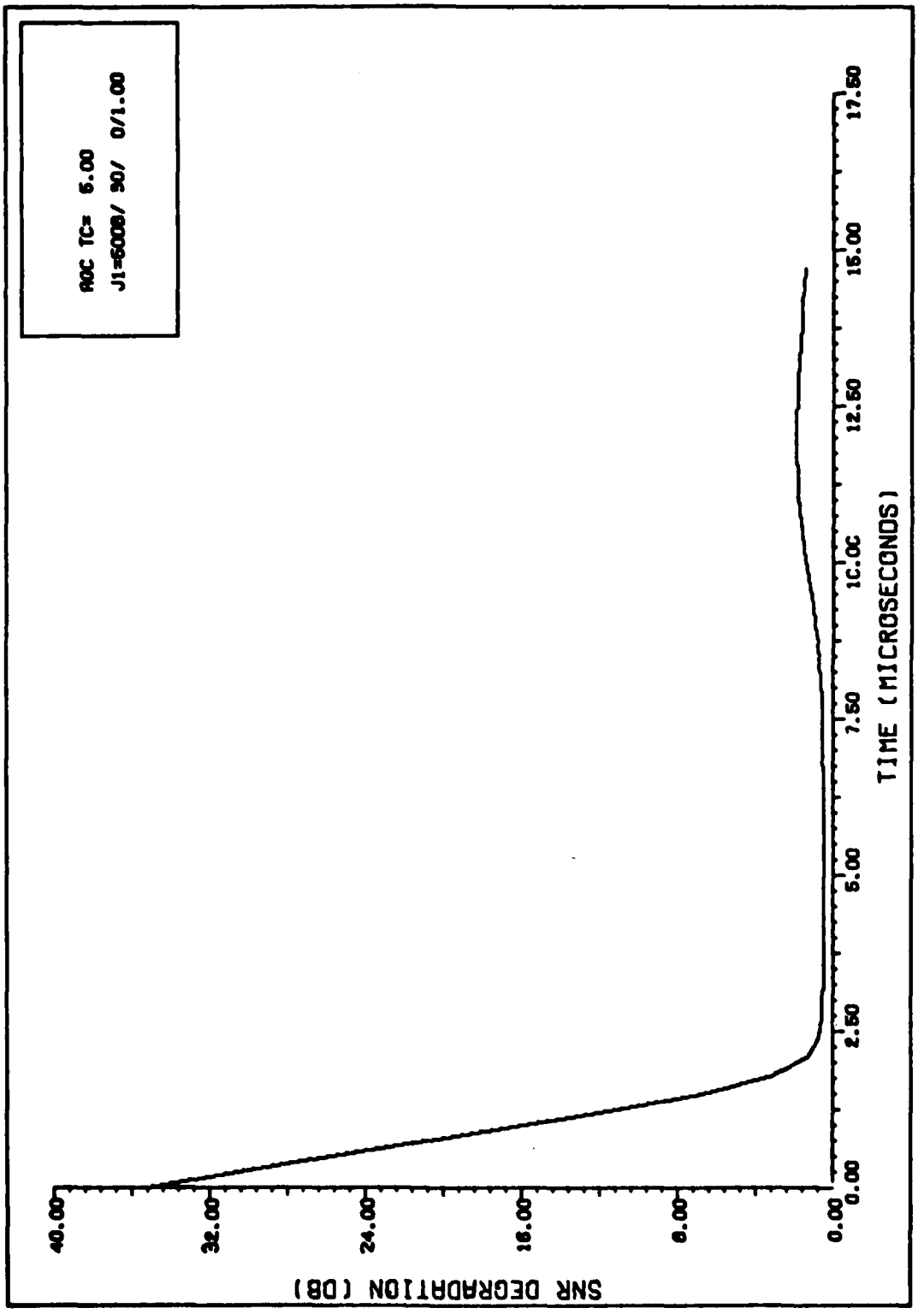

FIGURE 19. TRANSIENT DEGRADATION (CASE 9)

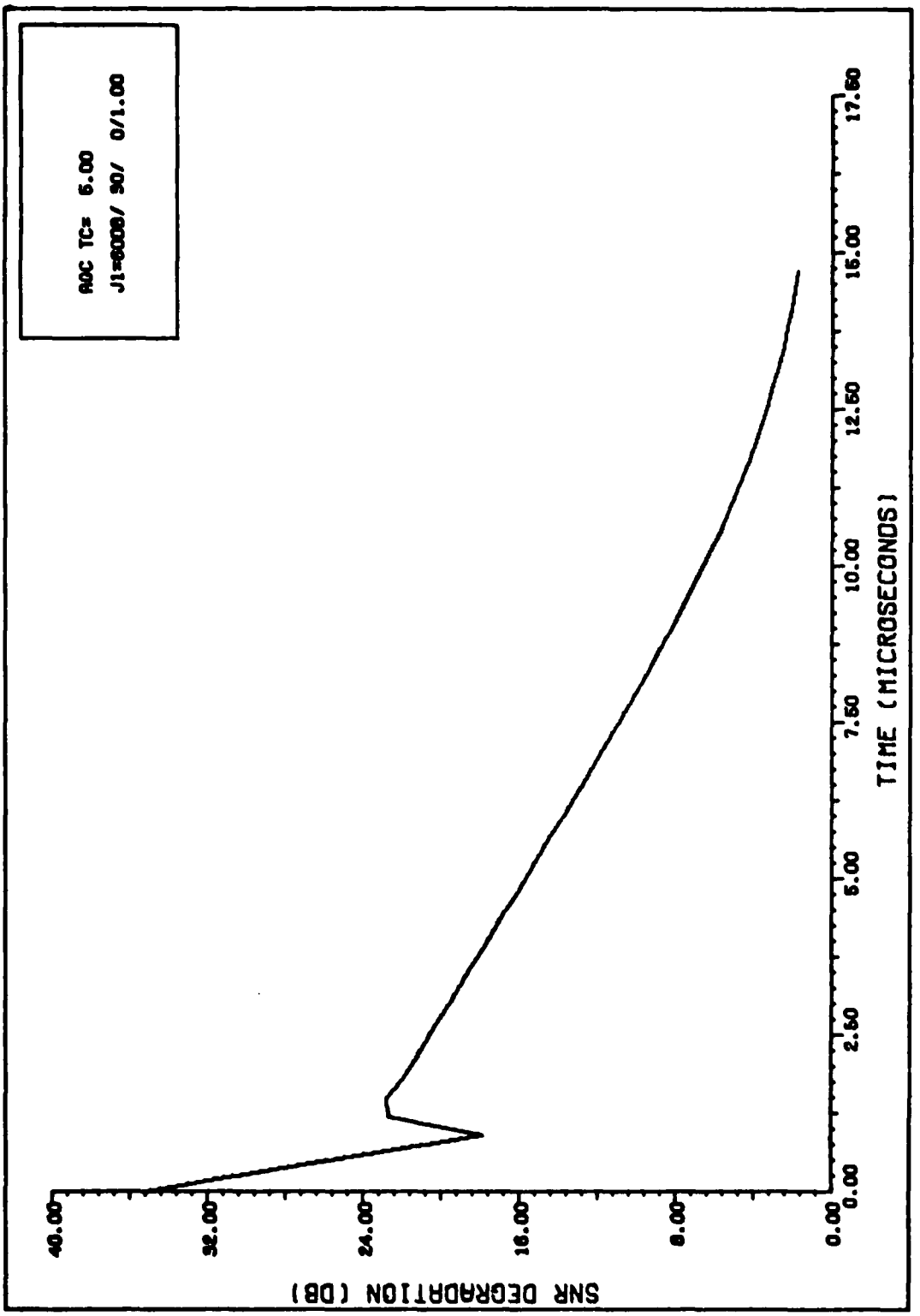

FIGURE 20. TRANSIENT DEGRADATION (CASE 10)

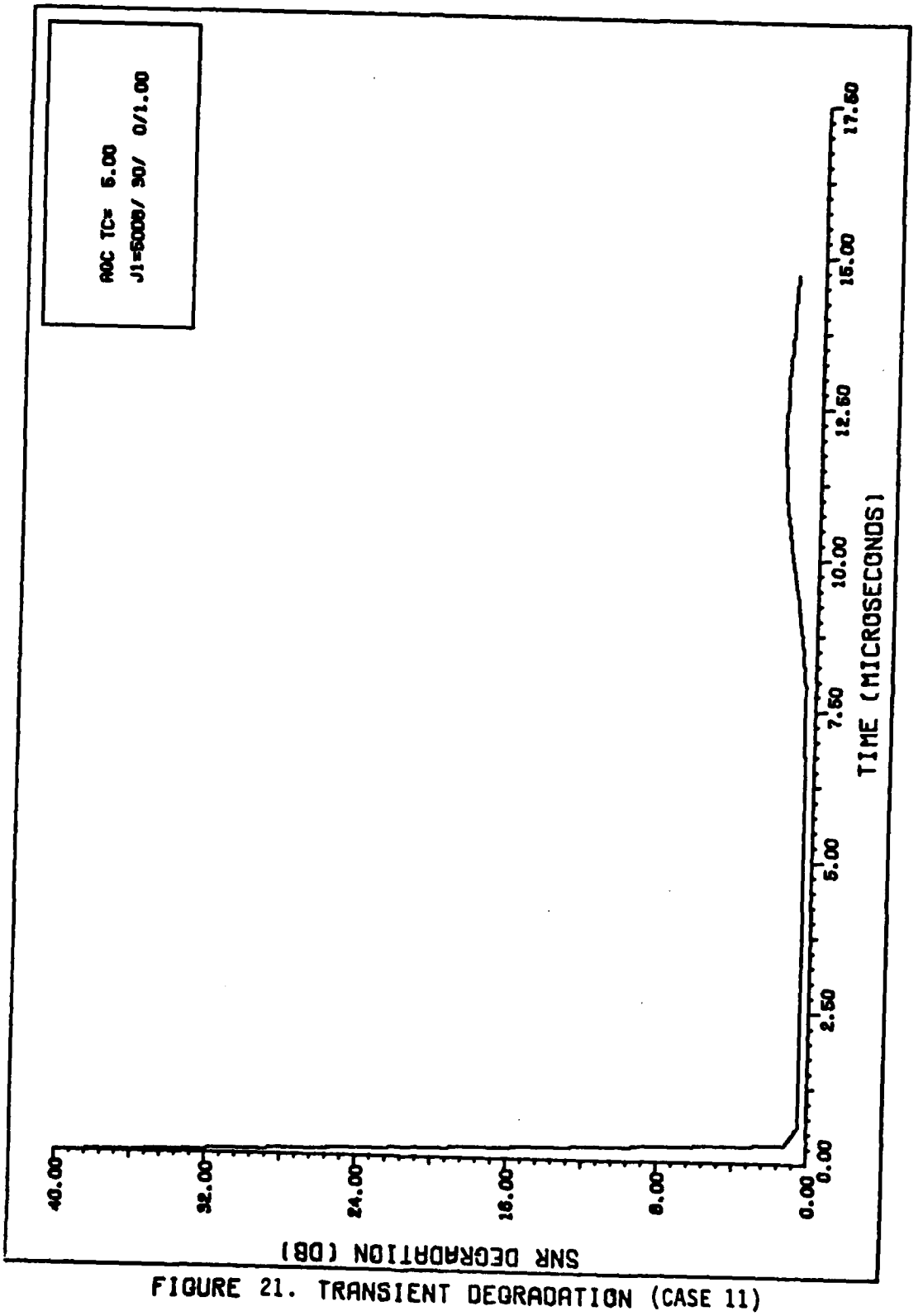

FIGURE 21. TRANSIENT DEGRADATION (CASE 11)

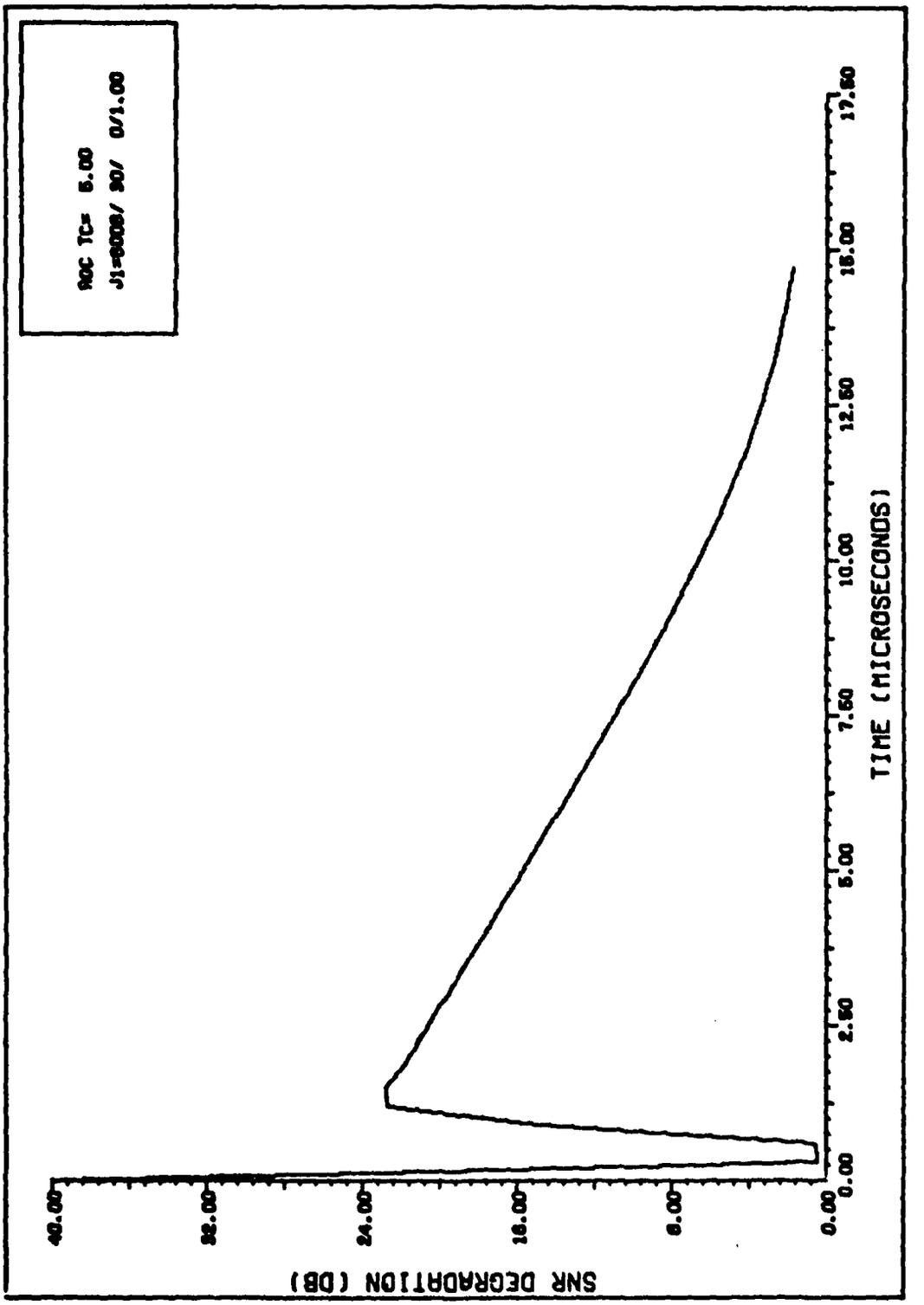

FIGURE 22. TRANSIENT DEGRADATION (CASE 12)

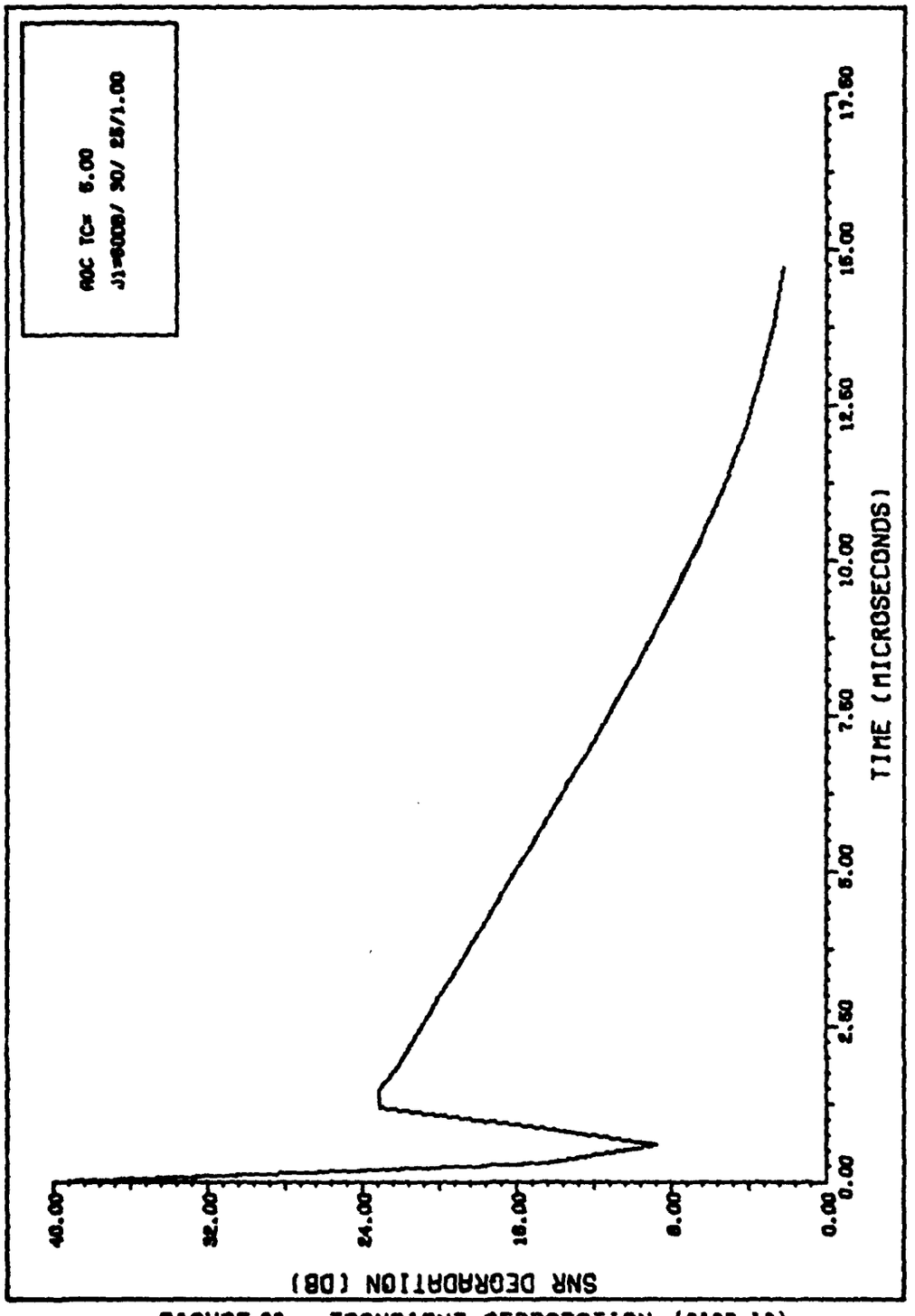

FIGURE 23. TRANSIENT DEGRADATION (CASE 13)

TABLE II

Case	Power (dBW)	Bandwidth (percent)	Spectral lines	Frequency ratio
9	50(s)	0	1	1.00
10	60(s)	0	1	1.00
11	50	0	1	1.00
12	60	0	1	1.00
13	60	25	20	1.00
14	60	50	40	1.00
15	60	50	40	1.00
16	50	10	20	.96
17	60	10	20	.96

center frequency. Hence, a deviation from the center is not faithfully represented by the phase factor. The weights generating the retrodirective beam beam are slightly off in phase and do not match the interference. Perhaps more important is the observation that increasing the bandwidth partially defeats any positive effects resulting from the use of an AGC. However, the period when the AGC has not reached its bias level is subject to interpretation. It is not difficult to imagine saturation giving rise to large intermodulation within the array. In keeping with the assumption neglecting intermodulation, it appears that this AGC transient period has beneficial side effects for the array. Cases 14 and 15, although unrealistic jammer

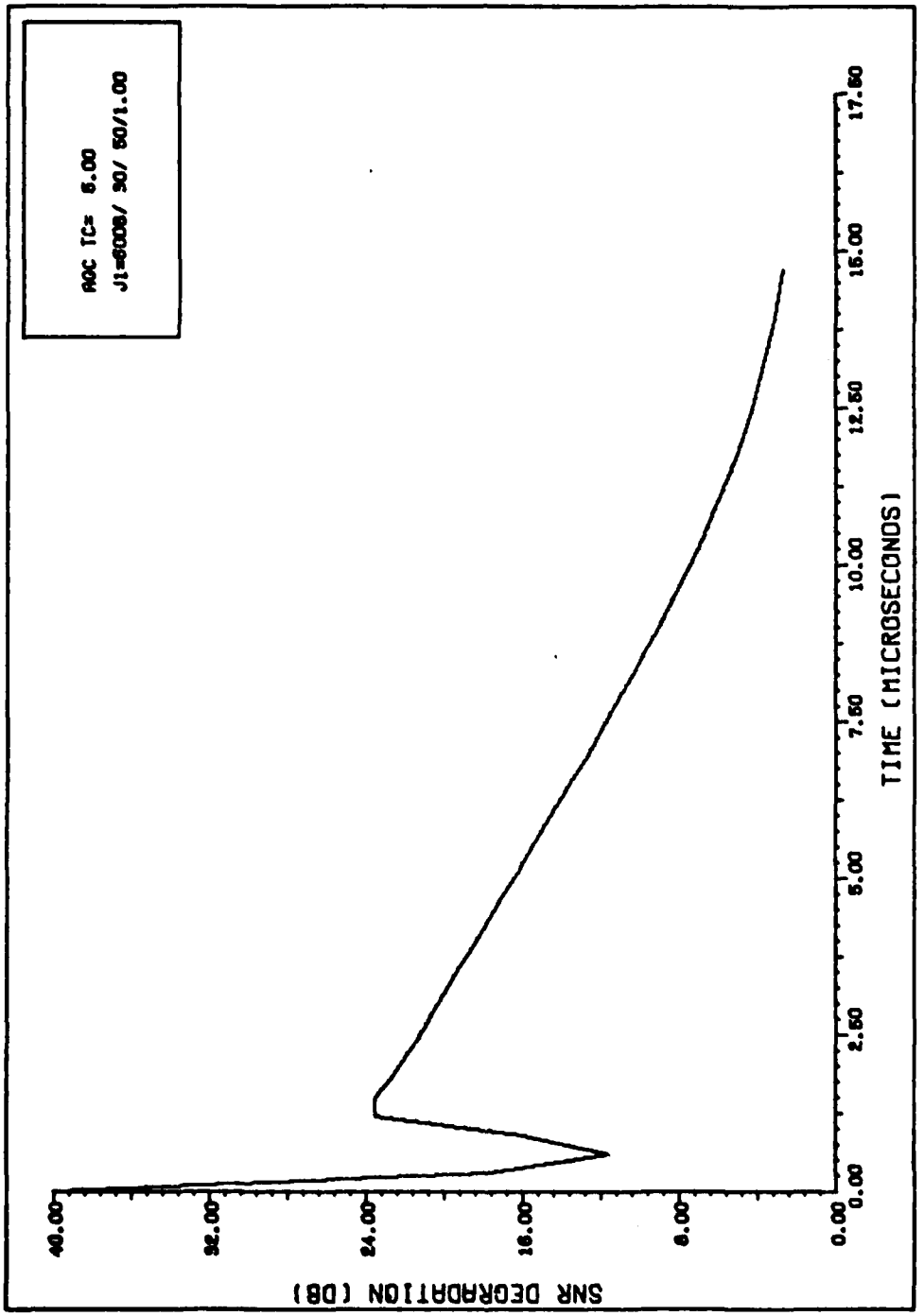

FIGURE 24. TRANSIENT DEGRADATION (CASE 14)

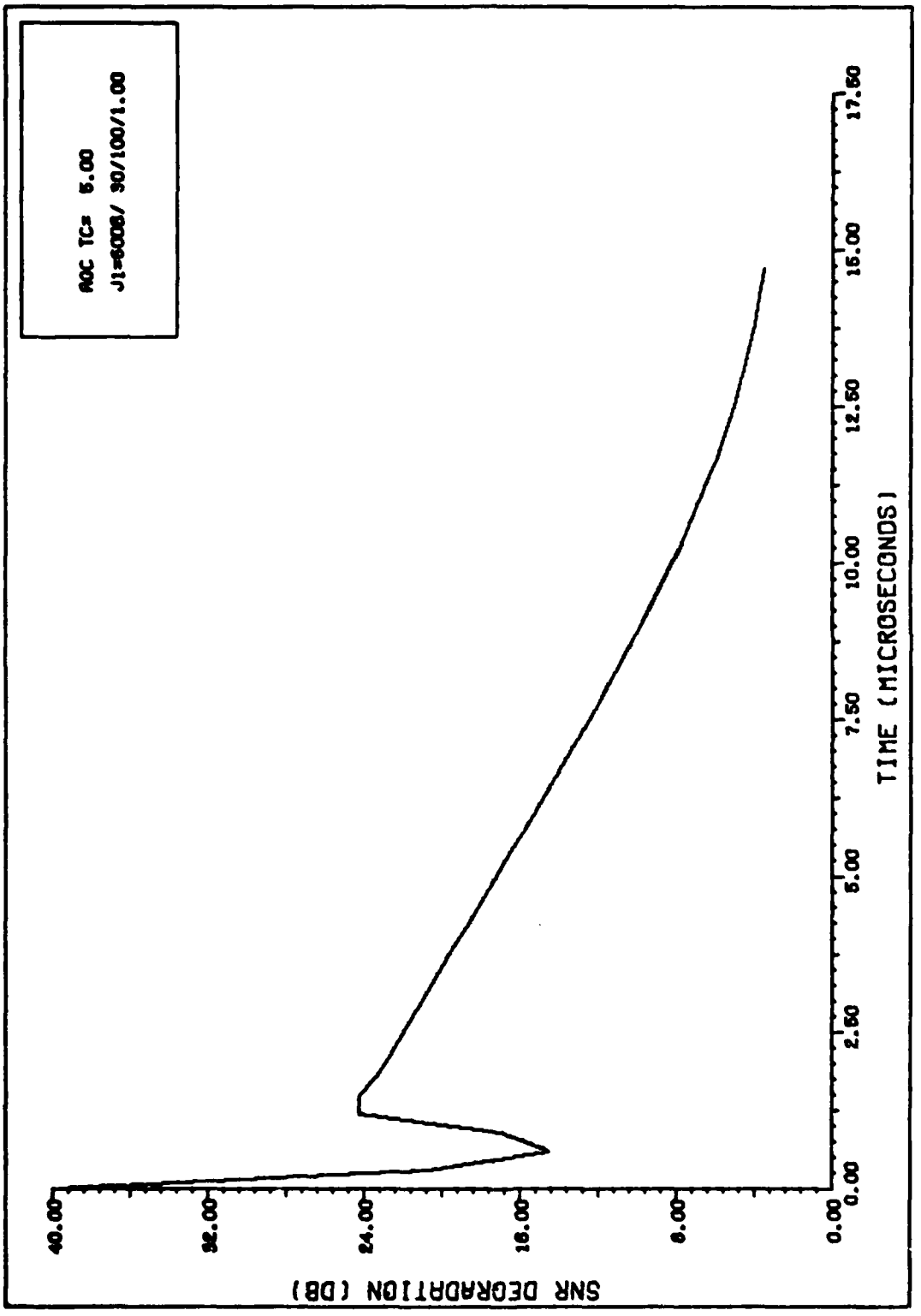

FIGURE 25. TRANSIENT DEGRADATION (CASE 15)

scenarios (5MHz Channel), further show this point. Cases 16 and 17 present plots which can be compared to cases 11 and 12 to see the effect of a 10 percent jammer bandwidth at the lower end of the channel. The fast change due to the AGC is seen to still exist, followed by a rise in SNR degradation. Again, the increase in degradation becomes asymptotic to case 1.

Case 12 also illustrates a previous claim that the adaptive weight amplitude varies significantly while the AGC is reaching the steady state level of 30dB. This amplitude variation has the effect of "moving" the null. The five antenna pattern plots (Figures 28 through 33) examine the first 1.8 microseconds of the transient response at .3 microsecond intervals. Initially, due to the large eigenvalue a deep null is placed on the jammer. However, as the AGC reaches steady state, the null moves back towards its quiescent location and continues this trend until the adaptive loop "catches up". This movement is specifically caused by the generation, collapse, and finally generation of the retrodirective beam the array is attempting to place on the jammer. This is not to be confused with adaptive weight phase changes which could possible produce similar results.

Results Summary. The major interesting result from the above comparisons is the "null movement" which can be traced directly to the AGC and its effect on the jammer power.

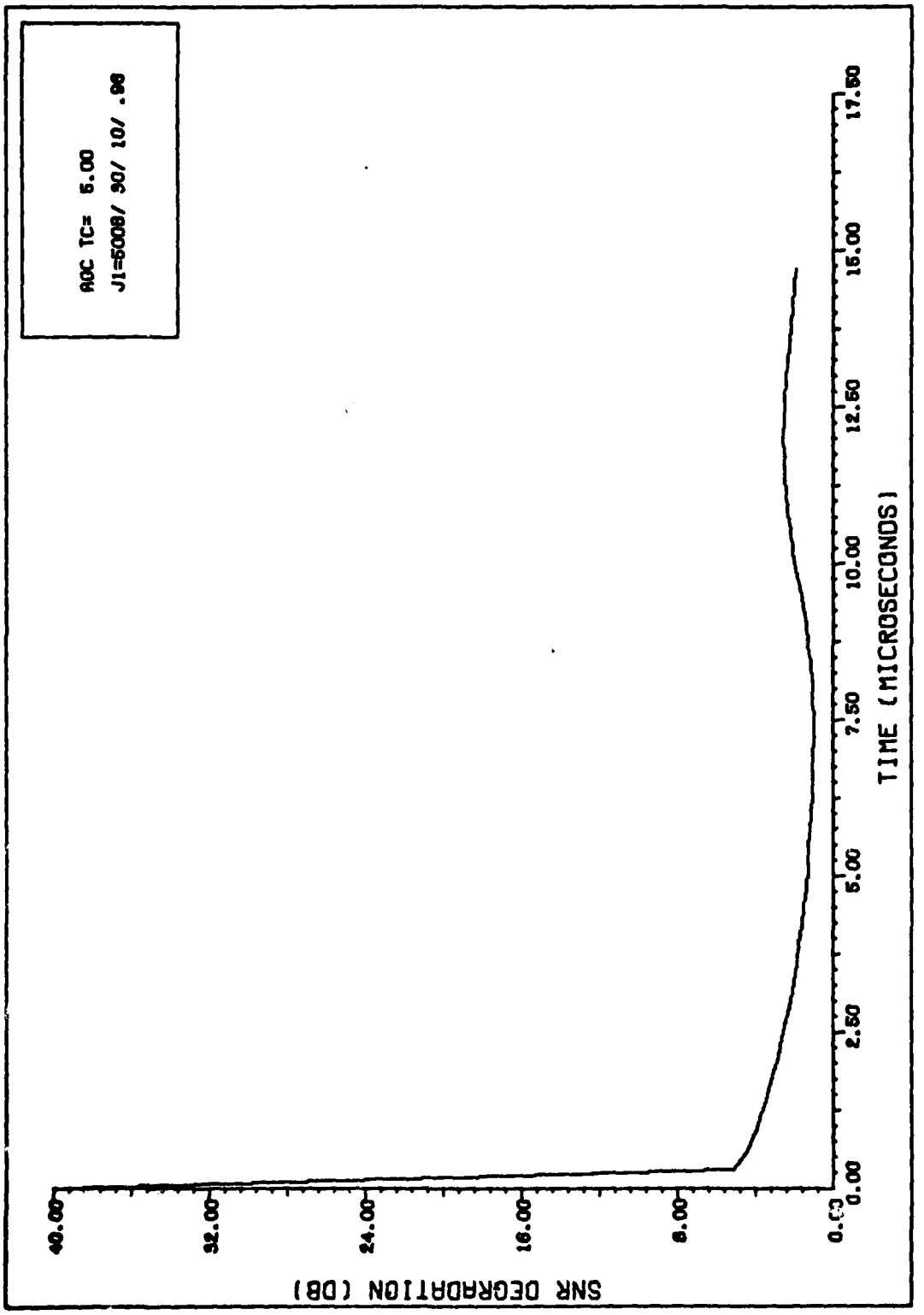

FIGURE 26. TRANSIENT DEGRADATION (CASE 16)

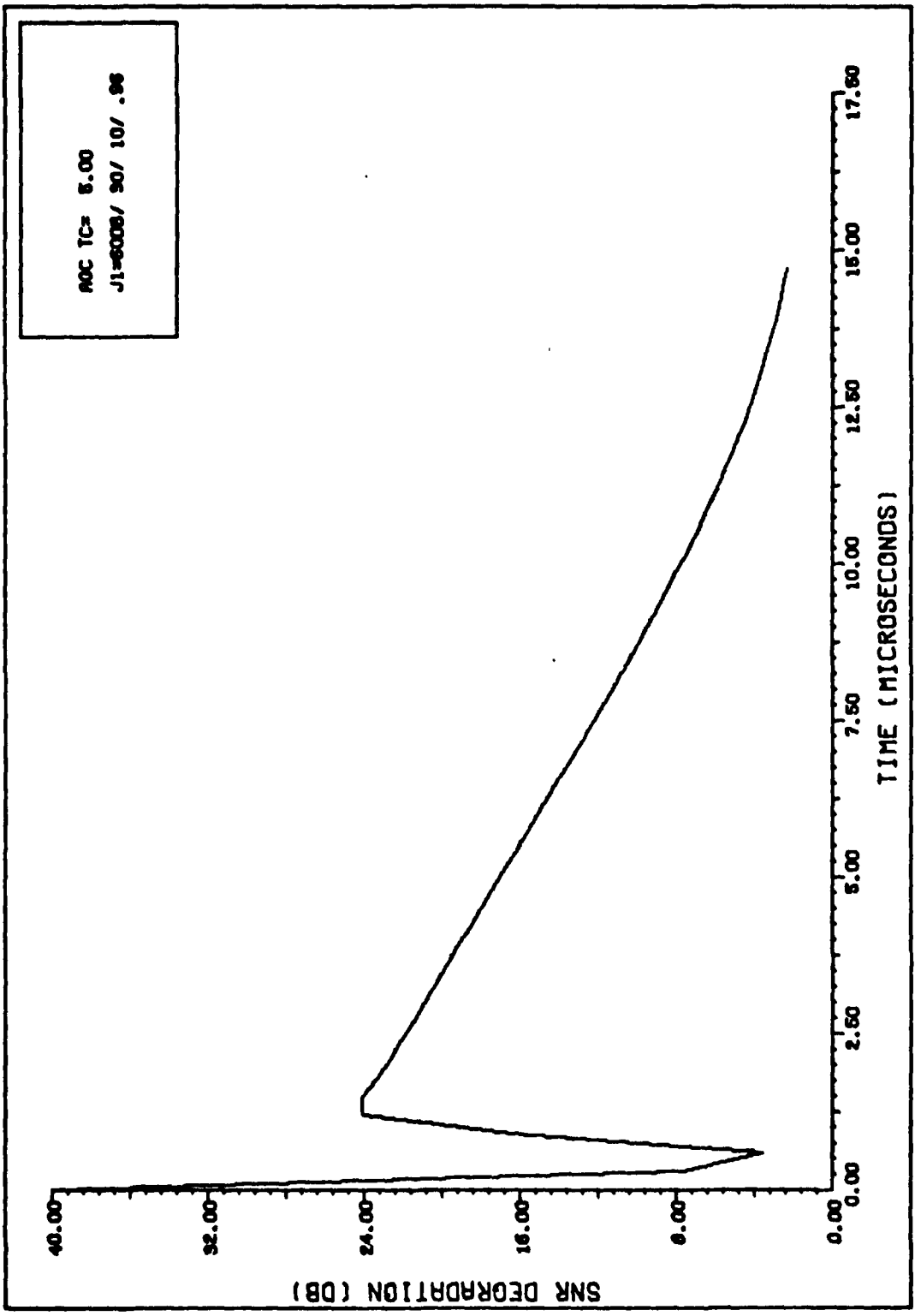

FIGURE 27. TRANSIENT DEGRADATION (CASE 17)

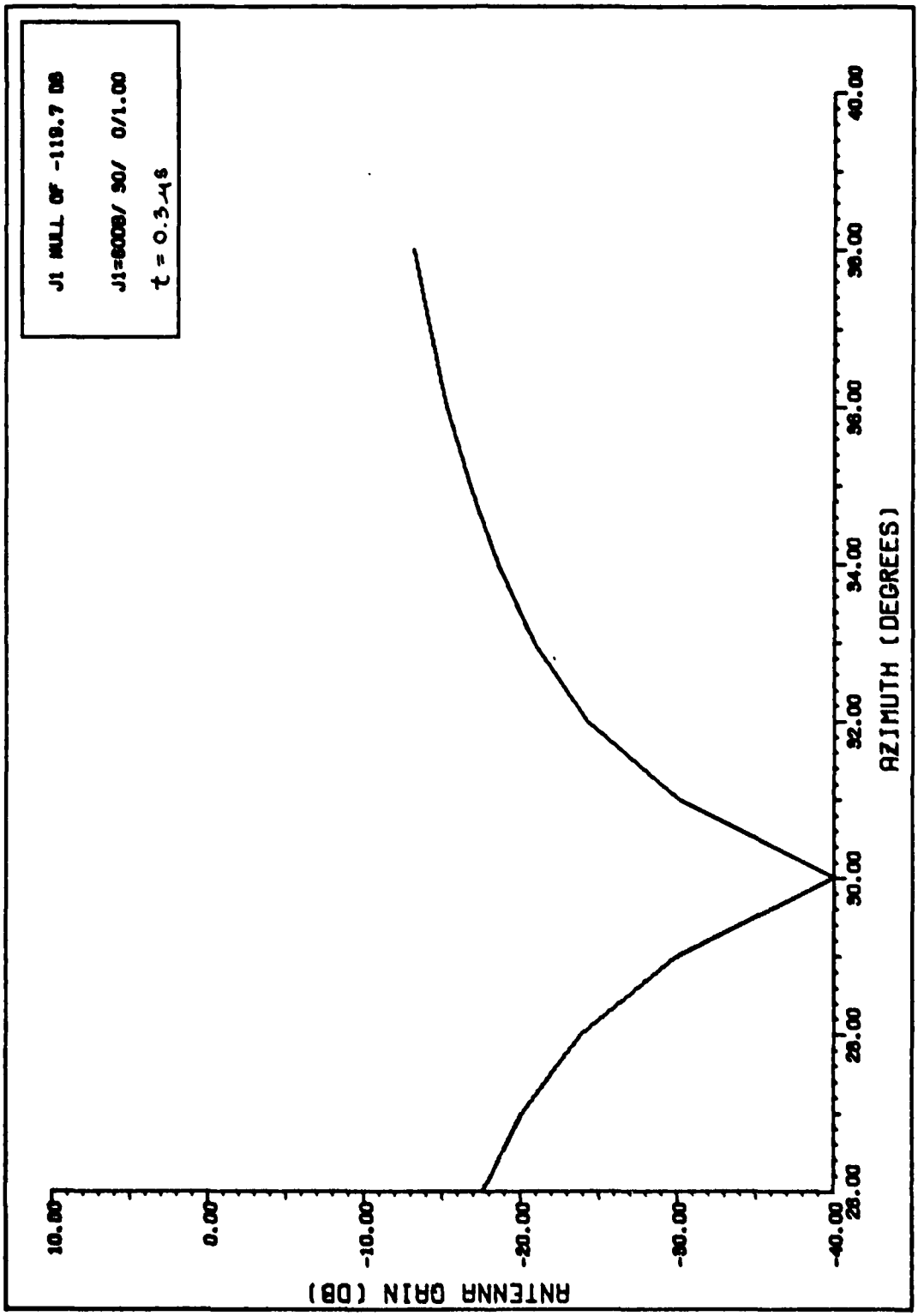

FIGURE 28. ADAPTED ANTENNA PATTERN (CASE 12)

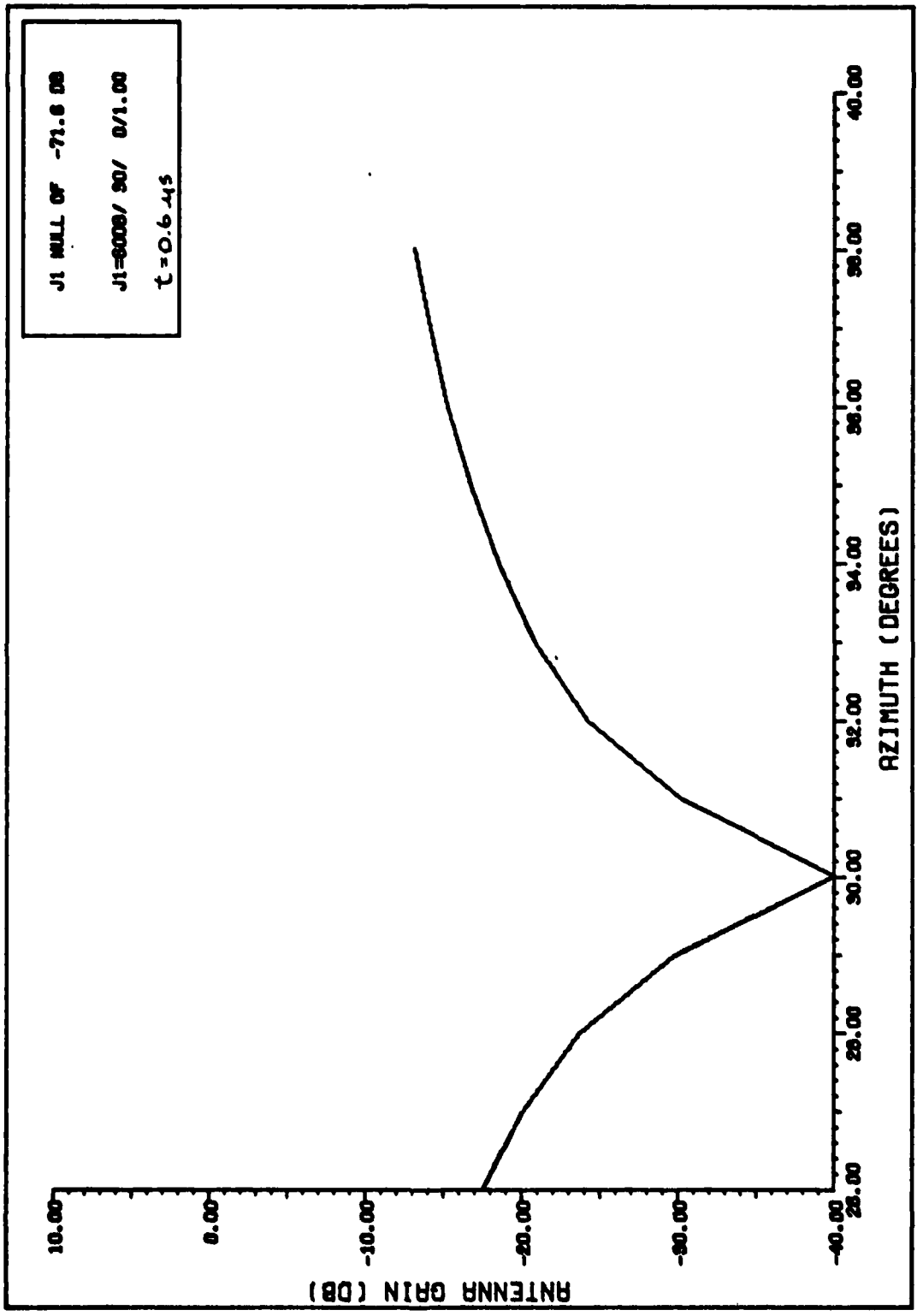

FIGURE 29. ADAPTED ANTENNA PATTERN (CASE 12)

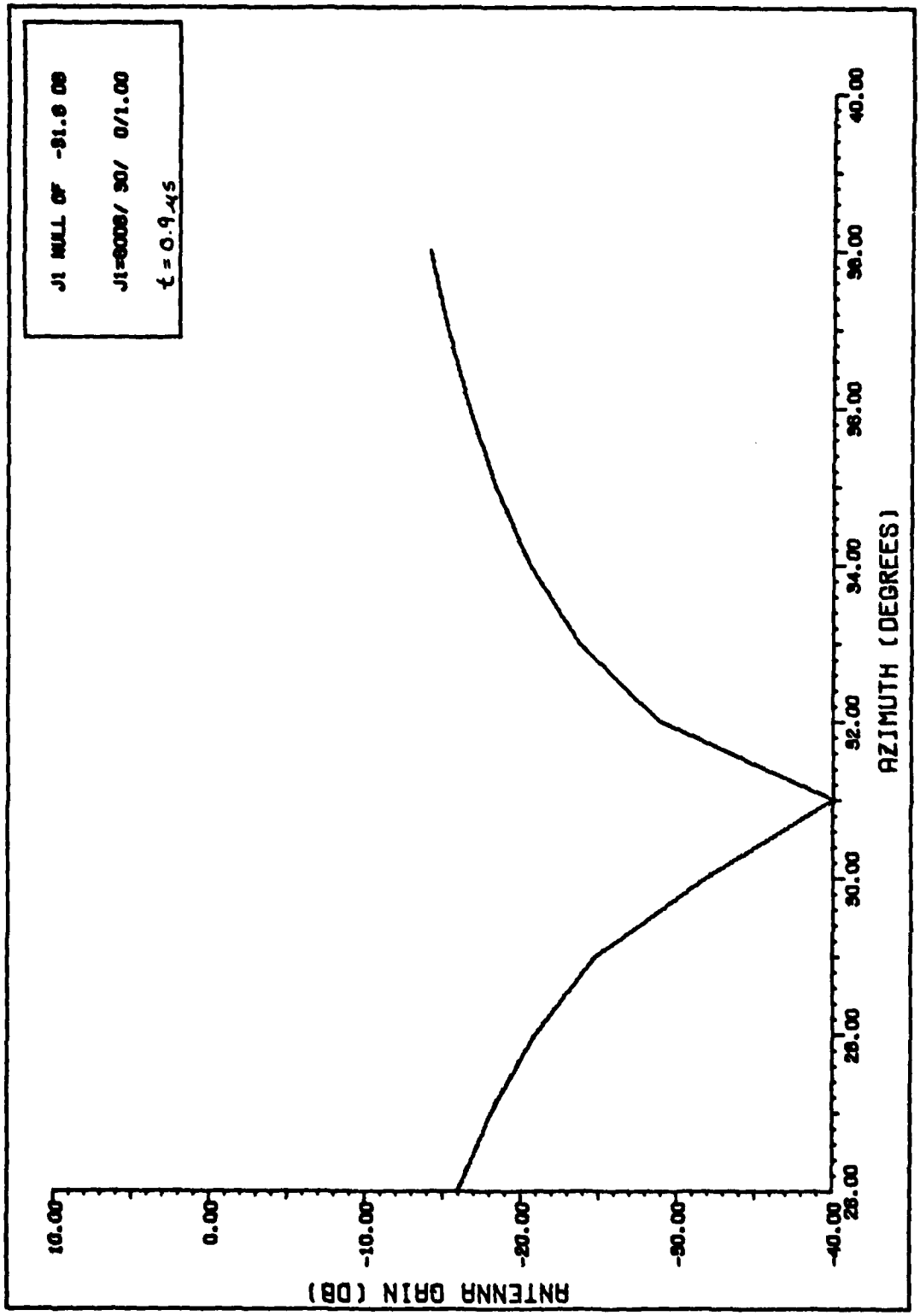

FIGURE 30. ADAPTED ANTENNA PATTERN (CASE 12)

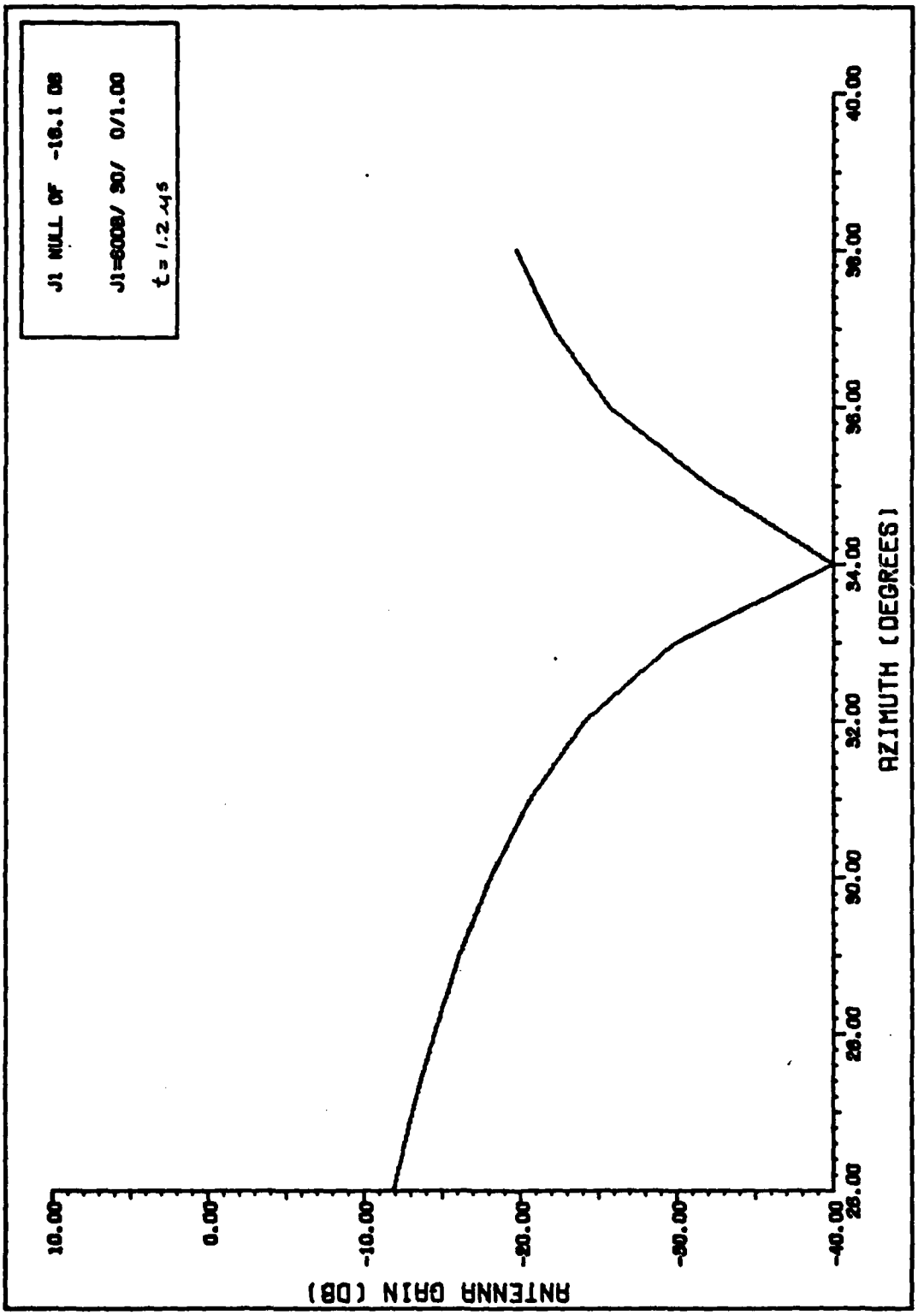

FIGURE 31. ADAPTED ANTENNA PATTERN (CASE 12)

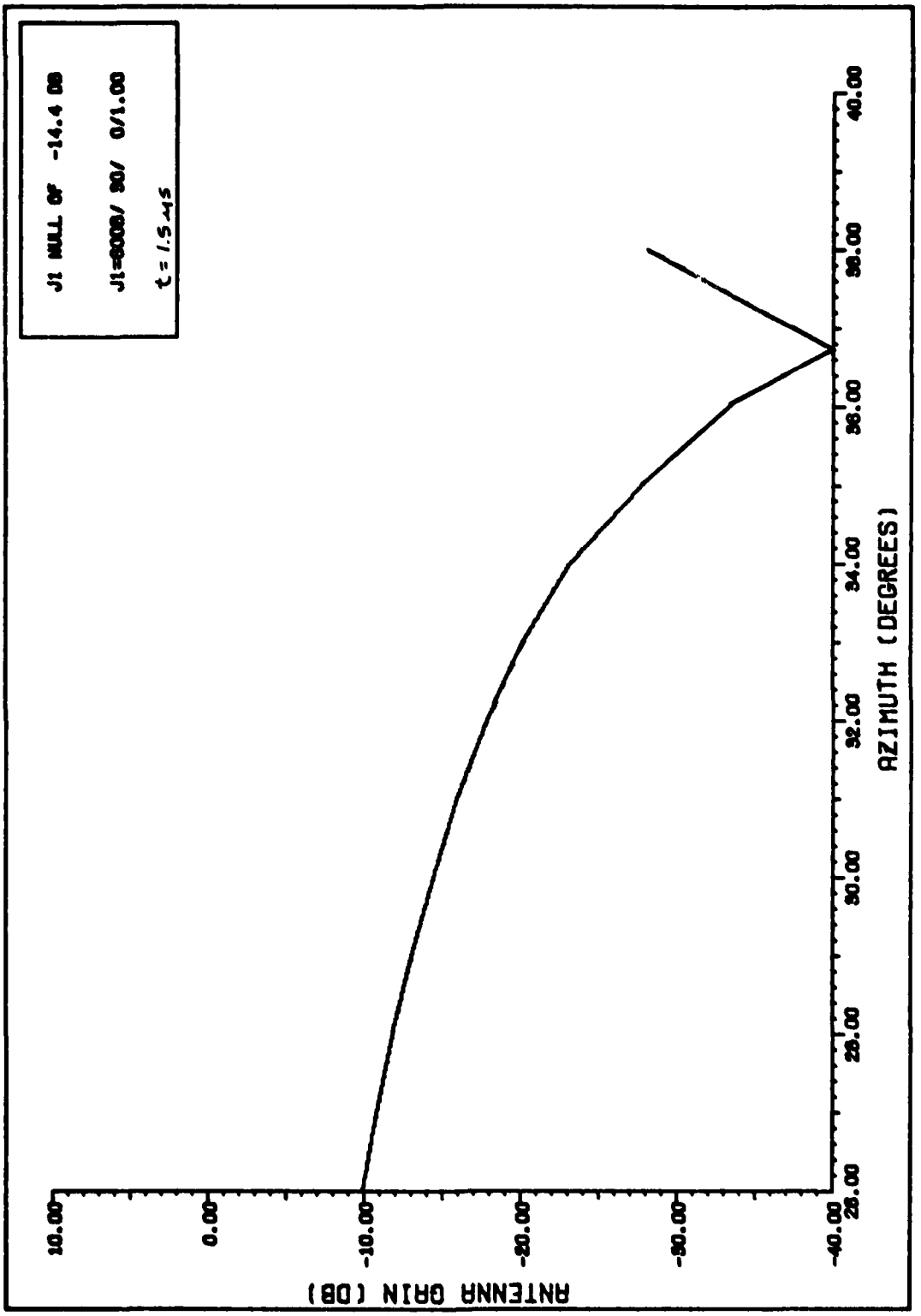

FIGURE 32. ADAPTED ANTENNA PATTERN (CASE 12)

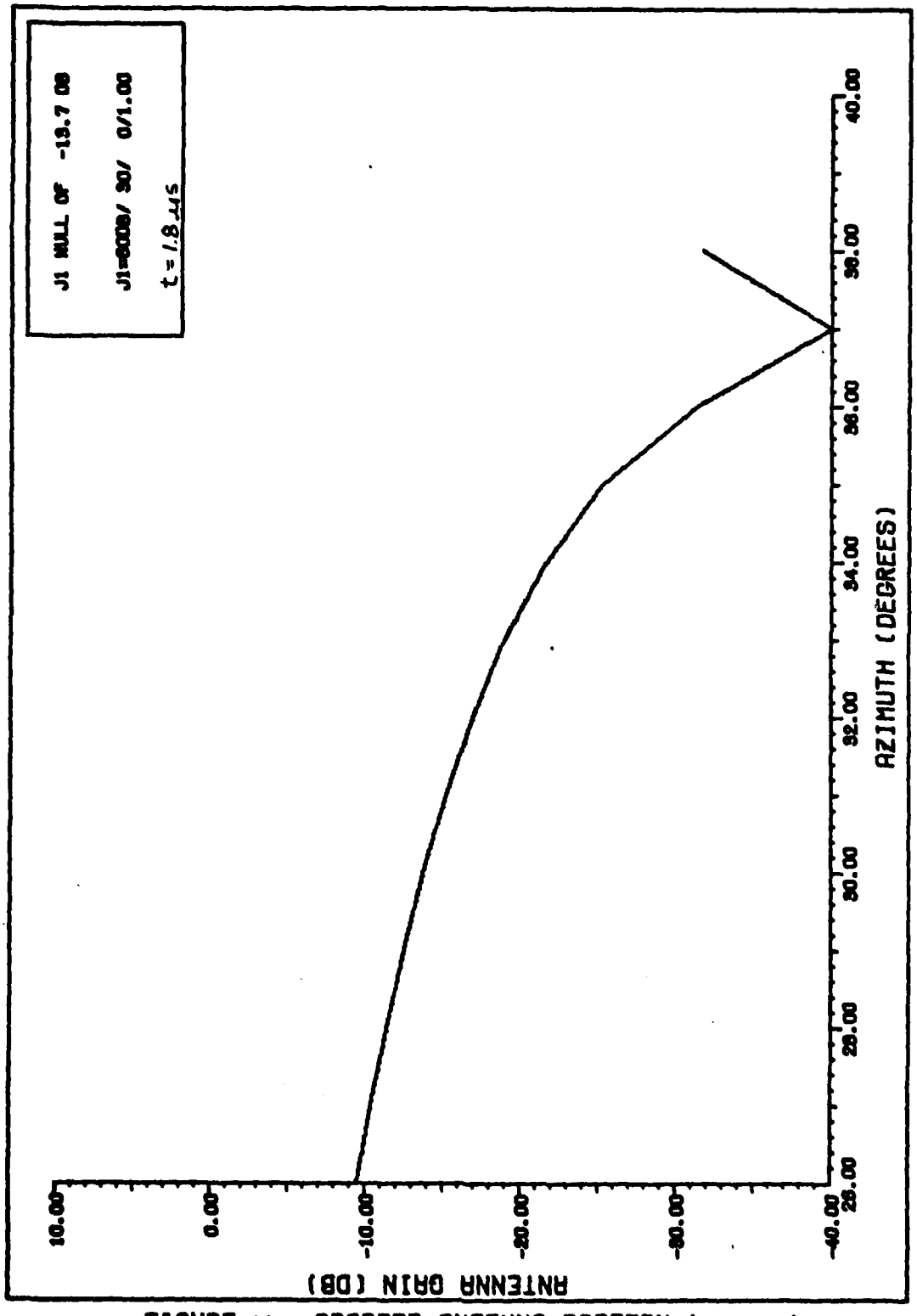

FIGURE 33. ADAPTED ANTENNA PATTERN (CASE 12)

Based upon the algorithm used it is seen that the power dependent eigenvalues are ultimately affected. It was also seen that a jammer with bandwidth increases the degradation during the period before AGC settling.

V. Conclusions and Recommendations

Conclusions

The preceeding section analyzed simulation results for an adaptive array with a linear AGC. Given that an adaptive array requires the use of AGC's for some reason, the following conclusions can be made.

1. Maximum average degradation is induced by high power, broadband interference in the cases where the AGC and array response times are similar.

2. When the response times are similar it is possible to "confuse" the array. This confusion is caused by inconsistent movement of the null; first in the direction of the interference, then back towards the quiescent position, and finally towards the interference. The typical monotonic movement is destroyed. High interference to noise ratios are not necessarily needed to cause this movement.

3. To reduce the effects of 1 and 2 above AGC's with large α values should be used.

However, if an AGC is required (chosen over a hard limiter perhaps) the implementation of 3 above implies the use of circuits with wide bandwidths. This may be of no consequence for spread spectrum systems. Narrowband systems, on the other hand, may not enjoy this option; design tradeoffs will have to be addressed. Even with "fast" AGC circuits

it is conceivable that a jammer could shape his interference (in time and frequency) to produce the effects shown in this thesis. In other words, he could force the AGC to operate "slower".

Recommendations

The following recommendations are given for future consideration.

1. Pulse jamming could conceivably cause severe SNR degradation of an AGC/array or simple array system. These systems have circuits of selected bandwidths with, of course, associated natural frequency specifications. Pulse jamming with the correct pulse duration and/or frequency relationships could affect these circuits to cause maximum resonant responses. These ideas should be investigated in the frequency domain with a "sync" function representation of the jammer.

2. Investigate the use of pulse shaping as a means of "slowing" the AGC response.

3. Compare and contrast AGC's with other envelope limiters to the state-of-the-art.

4. Cases 5 and 9 suggest that a proper choice of α can substantially decrease degradation. If this is the case, then AGC's with adaptive responses could further enhance adaptive array performance.

Bibliography

1. Howells, P.W. "Intermediate Frequency Side-Lobe Canceller," US Patent 3,202,990, 24 August 1965.

2. Applebaum, S.P. "Adaptive Arrays," Syracuse University Research Corp., Report SPL TR 66-1, August 1966. (Also IEEE Trans. Antennas and Propagation, AP-24(5):585-598 (September 1976).

3. Widrow, B. et al. "Adaptive Antenna Systems," Proceedings of the IEEE,(54):2143-2159 (December 1967).

4. Gabriel, W.F. "An Introduction to Adaptive Arrays," Naval Research Laboratory Report 7739, 31 July 1974 (Shortened version in IEEE Proceedings, Vol 64, no.2, February 1976.) (DDC AD922178L).

5. Brennan, L.E. and I.S. Reed. "Effect of Envelope Limiting in Adaptive Array Control Loops," IEEE Trans. Aerospace Electronic Systems, AES-7: 698-700 (July 1971).

6. Weeks, W.L. Antenna Engineering, New York: McGraw-Hill Book Co., 1968.

7. Ziemer, R.E. and W.K. Tranter. Principles of Communications, Boston: Houghton Mifflin Co., 1976.

8. Papoulis, A. Probability, Random Variables, and Stochastic Processes, New York: McGraw-Hill Book Co., 1965.

9. Wozencraft, John M. and Irwin M. Jacobs. Principles of Communication Engineering, New York: Wiley and Sons, Inc., 1967.

10. Oliver, B.M. "Automatic Volume Control as a Feedback Problem," Proceedings of the IRE:466-473 (April 1948).

11. Victor, W.K. and M.H. Brockman. "The Application of Linear Servo Theory to the Design of AGC Loops," Proceedings of the IRE:234-238 (February 1960).

12. Banta, E.D. "Analysis of an Automatic Gain Control (AGC)," IEEE Trans. Automatic Control, AC-9:181-182 (April 1964).

13. Plotkin, S. "On Nonlinear AGC," Proceedings of the IEEE: 380 (February 1963).

14. Gill, W.J. and W.K.S. Leong. "Response of an AGC Amplifier to Two Narrow-Band Input Signals," IEEE Trans. Communications Technology, COM-14(4):407-417(August 1966).

15. Ohlson, J.E. "Exact Dynamics of Automatic Gain Control," IEEE Trans. Communications: 72-74 (January 1974).

Vita

John Rogers Sutton was born on 21 February 1953. He graduated from high school in Seneca Falls, New York in 1971 and attended the United States Air Force Academy, receiving a Bachelor of Science degree in Electrical Engineering in June 1975. Upon graduation, he attended the Communications-Electronics Engineer School at Keesler AFB, Mississippi. From March 1976 to May 1978 he served as a communications engineer for the 507th Tactical Air Control Wing, Shaw AFB, South Caroline. In June 1978 he entered the Air Force Institute of Technology Masters degree program.

AD-A080 374 AIR FORCE INST OF TECH WRIGHT-PATTERSON AFB OH SCHOOL--ETC F/G 17/4
AN ADAPTIVE ARRAY WITH AUTOMATIC GAIN CONTROL.(U)
DEC 79 J R SUTTON
UNCLASSIFIED AFIT/GE/EE/79-36 NL

2 OF 2
AD A080374

END
DATE FILMED
3-80
DDC

UNCLASSIFIED
SECURITY CLASSIFICATION OF THIS PAGE (When Data Entered)

REPORT DOCUMENTATION PAGE		READ INSTRUCTIONS BEFORE COMPLETING FORM
1. REPORT NUMBER GE/EE/79-36	2. GOVT ACCESSION NO.	3. RECIPIENT'S CATALOG NUMBER
4. TITLE (and Subtitle) An Adaptive Array with Automatic Gain Control		5. TYPE OF REPORT & PERIOD COVERED MS Thesis 6. PERFORMING ORG. REPORT NUMBER
7. AUTHOR(s) John P. Sutton CAPT USAF		8. CONTRACT OR GRANT NUMBER(s)
9. PERFORMING ORGANIZATION NAME AND ADDRESS Air Force Institute of Technology (AFIT/EN) Wright-Patterson AFB, Ohio		10. PROGRAM ELEMENT, PROJECT, TASK AREA & WORK UNIT NUMBERS
11. CONTROLLING OFFICE NAME AND ADDRESS RADC/DCID Griffiss AFB, NY		12. REPORT DATE Dec 1979 13. NUMBER OF PAGES 97
14. MONITORING AGENCY NAME & ADDRESS(if different from Controlling Office)		15. SECURITY CLASS. (of this report) UNCLAS 15a. DECLASSIFICATION/DOWNGRADING SCHEDULE

16. DISTRIBUTION STATEMENT (of this Report)

Approved for Public Release; distribution unlimited.

17. DISTRIBUTION STATEMENT (of the abstract entered in Block 20, if different from Report)

18. SUPPLEMENTARY NOTES

Approved for Public Release; IAW AFR 190-17

J. P. Hipps, Major, USAF
Director of Public Affairs

19. KEY WORDS (Continue on reverse side if necessary and identify by block number)

Adaptive Arrays
Antenna Arrays
Adaptive Antenna Arrays

20. ABSTRACT (Continue on reverse side if necessary and identify by block number)

A three-element adaptive array algorithm with Applebaum-Howells loops combined with a linear automatic gain control (AGC), was analyzed. Computer simulations of array performance for signal jammers were presented and analyzed. Jammer scenarios included were: narrowband and broadband, high power, centered and non-centered jammers about the array center frequency, and different automatic gain control response times. No fixed performance criteria were applied to SNR degradation and antenna pattern plots. A non-linear

DD FORM 1 JAN 73 1473 EDITION OF 1 NOV 65 IS OBSOLETE

UNCLASSIFIED
SECURITY CLASSIFICATION OF THIS PAGE (When Data Entered)

linearized by expanding the exponential attenuation functio
ies and truncating the higher-order terms. The AGC is shown
oy the typical monotonically decreasing SNR degradation of
nt power, narrow band jammer when its response time is near
the adaptive loop. Simulation results show that an AGC can
e adaptive weight amplitudes to vary significantly.